

**A Comparative Design Study for Gas Turbine Regulation using
Least Effort Control**

دراسة مقارنة للتحكم بمحرك الغاز التوربيني باستخدام نظام التحكم ذي الجهد المنخفض

by

EYAD MEGDADI

**A dissertation submitted in fulfilment
of the requirements for the degree of
MSc Systems Engineering
at
The British University in Dubai**

**Prof. R. Whalley
May 2017**

DECLARATION

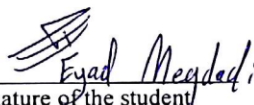
I warrant that the content of this research is the direct result of my own work and that any use made in it of published or unpublished copyright material falls within the limits permitted by international copyright conventions.

I understand that a copy of my research will be deposited in the University Library for permanent retention.

I hereby agree that the material mentioned above for which I am author and copyright holder may be copied and distributed by The British University in Dubai for the purposes of research, private study or education and that The British University in Dubai may recover from purchasers the costs incurred in such copying and distribution, where appropriate.

I understand that The British University in Dubai may make a digital copy available in the institutional repository.

I understand that I may apply to the University to retain the right to withhold or to restrict access to my thesis for a period which shall not normally exceed four calendar years from the congregation at which the degree is conferred, the length of the period to be specified in the application, together with the precise reasons for making that application.


Signature of the student

Abstract

This study investigates gas turbine engine regulation for heavy duty vehicles using least effort and H infinity control strategies to evaluate the system response, performance and consumption of power. This research study shows how the least effort control gives good transient response, with characteristics of output decoupling and disturbance rejection using a simple feedback strategy. It is shown that the least effort controller gives minimum control energy consumption which causes least heat and power losses and lower maintenance cost. A comparison study with the H infinity method was conducted, to show the advantages and disadvantages of each method. The system model investigated used the linearized equations for an automotive gas turbine, to obtain the vehicle, high load response. The fuel flow and nozzle area of the gas turbine, are used as reference inputs to control the change in the model gas stream temperature, and angular velocity, as system outputs.

خلاصة الأطروحة

في هذا البحث يتم دراسة التحكم في محركات الغاز التوربينية للأليات الثقيلة باستخدام طريقة الطاقة المنخفضة وطريقة اتش اللانهائية لتنظيم استجابة النظام , مع التركيز على الاداء و الطاقة المستهلكة . وتبين هذه الدراسة البحثية كيف تعطي طريقة التحكم ذات الطاقة المنخفضة استجابة جيدة للنظام مع خصائص فصل ارتباط مخرجات النظام و الحد من تأثير الاضطرابات و التشويش, باستخدام نظام تحكم بسيط بالتغذية الراجعة. وتبين هذه الدراسة البحثية كيف تعطي طريقة التحكم ذات الطاقة المنخفضة أقل مستوى للطاقة اللازمة للتحكم و التي تؤدي إلى تقليل الحرارة و ضياع الطاقة في النظام و تقليل التكلفة اللازمة للصيانة. و في هذا البحث تم انجاز دراسة مقارنة مع طريقة اتش اللانهائية لتنظيم استجابة النظام لإظهار حسنات و مساوى كل من الطرق المستخدمة. و تم اختبار نموذج النظام باستخدام معادلات خطية لمحرك الغاز التوربيني للأليات لتعكس استجابة الألية. و في هذا البحث تم استخدام تدفق الوقود و حجم فوهة الهواء لمحرك الغاز التوربيني كمدخلات مرجعية للتحكم في التغيير في حرارة تيار الغاز المحول و السرعة الزاوية و مخرجات النظام.

Acknowledgments

My special thanks and gratitude to Professor Robert Whalley for the full support and guidance he provided during my study at the British University in Dubai. Also I want to extend my thanks to Dr. Alaa Ameer for assistance that he provided during my study and all the staff and management personnel at the British University in Dubai for their enthusiastic and dedicated work.

Dedication

To my father and mother who believed in me.

To my wife who gave me full support.

To all the people who advised me in my life.

To my colleagues in BUiD who shared my experience at in BUiD.

I dedicate my work to all of you.

List of notation

$A(s)$	Numerator of $G(s)$	matrix
$a_{ij}(s)$	Element of $A(s)$	function
$a_{ij}, b_{ij}, \dots, \gamma_{ij}$	Coefficients of $a_{ij}(s)$	scalar
$b(s)$	Polynomial	function
b_0	Leading coefficient of $b(s)$	scalar
$d(s)$	Denominator of $G(s)$	function
$f(s)$	Transformed fuel flow signal	scalar
f	Outer loop gain	scalar
$G(s)$	Transfer function array for analysis	matrix
$g_{ij}(s)$	Elements of $G(s)$,	function
$h_j(s)$	Feedback path compensator	function
I	Identity matrix	matrix
J	Performance index	functional
k_1, k_2, \dots, k_m	Gains of $k_j(s)$, $1 \leq i, j \leq m$	scalar
h_1, h_2, \dots, h_m	Gains of $h_j(s)$, $1 \leq i, j \leq m$	scalar
$L(s)$	Left row factors	matrix
m	Number of inputs and outputs	scalar
$n(s)$	transformed nozzle actuator signal	scalar
n_1, n_2, \dots, n_{m-1}	Gain ratios	scalar
$P(s)$	Pre-compensator	matrix
Q	Coefficient array	matrix

$R(s)$	Right column factors	matrix
r_1, r_2	Reference inputs	scalar
$T(s)$	Gas temperature signal	scalar
$\omega(s)$	Gas turbine speed signal	scalar
$u(s)$	Input	vector
$y(s)$	Transformed output	vector
$\Gamma(s)$	Finite time delays	matrix
κ	Degree of $d(s)$	scalar
τ	Gas turbine time constant	scalar
$\delta(s)$	Disturbances	vector
i, j	Subscripts	scalar

List of Figures:

Figure		Page
Figure 1.1	general gas turbine schematic	11
Figure 1.2	gas turbine with electric generator for electric drive vehicles	13
Figure 2.1	diagram of gas turbine basic control system	17
Figure 2.2	diagram of water level regulator system.(Dorf and Bishop, 2011)	19
Figure 2.3	diagram of flyball governor system.(Dorf and Bishop, 2011)	20
Figure 2.4	process of open loop controller: a) System to be controlled. b) Open loop controller	22
Figure 2.5	process of feedback controller	23
Figure 2.6	PID controller representation	24
Figure 2.7	representation of a multivariable system	26
Figure 2.8	feedback regulating block diagram of multivariable system	27
Figure 2.9	rearrangement of feedback regulating block diagram of multivariable system	27
Figure 2.10	representing block diagram of state space modeling	30
Figure 2.11	representing block diagram of state space modeling with feedback gain	30
Figure 2.12	Optimal controller feedback gain diagram.	32
Figure 3.1	Diagram of gas turbine connected electric power system	36
Figure 3.2	The actual gas turbine model with reduced transfer functions	38
Figure 3.3	system response after applying a 1% unity step change in Fuel Pump % f_p	39
Figure 3.4	system response after applying a 1% unity step change in Guide Vane Unit % n_a	40
Figure 4.1	Feedback control structure typical	47
Figure 4.2	general structure of feedback control	48
Figure 4.3	structure of feedback control problem with weighting functions	49
Figure 5.1	root locus of the equation (5.4)	53
Figure 5.2	performance index with the gain ratio graph	56

Figure 5.3	closed loop system representation	58
Figure 5.4	conventional closed loop system representation	59
Figure 6.1	System response after applying a unit step change at $r_1(s)$	63
Figure 6.2	System response after applying a unit step change at $r_2(s)$	63
Figure 6.3	System response after applying a negative unit step at $\delta_1(s)$	64
Figure 6.4	System response after applying a negative unit step at $\delta_2(s)$	65
Figure 6.5	System response after applying a unit step change at $r_1(s)$	66
Figure 6.6	System response after applying a unit step change at $r_2(s)$	66
Figure 6.7	System response after applying a negative unit step at $\delta_1(s)$	67
Figure 6.8	System response after applying a negative unit step at $\delta_2(s)$	67
Figure 7.1	Least effort and H infinity controllers' energy dissipation.	70
Figure A.1	least effort controller simulation model	93
Figure A.2	H-infinity controller simulation model	97

List of Tables:

Table		Page
Table 2.1	Important developments of control science.(Dorf and Bishop,2011)	21
Table 5.1	The results obtain from MatLab application for the synthesis of H-infinity optimal controller.	60

Research Index:

Abstract	1
خلاصة الأطروحة	2
Acknowledgements	3
Dedication	4
List of notation	5
List of figures	7
List if tables	8
Index	9
1. Section one: Introduction	11
1 Background:	11
2 Problem statement:	14
3 Aims and objectives	15
4 Research Organization	15
2. Section two: Literature Review	17
1 Introduction	17
2 Control strategies review	18
3 Classical control theory	21
4 The British control school	25
5 The American control school	28
6 Main issues and concepts of control theory	33
7 The control methods used in this research	34
3. Section three: Research Methodology	36
1 Gas turbine modeling	36
2 Open loop response:	39
3 Controller methods	41

4	Section four: Control theory	42
1	Least effort controller theory	42
2	H infinity controller theory	47
5	Section five: Controller Design	51
1	Design of least effort controller	51
2	Design of H infinity controller	59
6	Section six: Simulation	62
1	Least effort controller simulation	62
2	H infinity controller simulation	65
7	Section seven: Comparison Study	69
1	Control energy consumption	69
2	Controller implementation	71
3	Disturbance rejection	71
8	Section eight: Conclusions and Recommendations	72
1	Conclusions	72
2	Recommendations	73
	References	74
	Appendix	79

Section one:

Introduction:

1.1 Background:

Gas turbine engines are widely used in industrial applications because of reliability, power weight ratio and their efficiency characteristics particularly for full load, constant speed applications. The excellent efficiency, compactness and high power-weight ratio characteristics of gas turbines are instrumental in their selection for industrial, maritime and aviation applications. Gas turbine prime movers were introduced in 1930. A successfully flight using Whittle's engine results in aerospace sector applications which continue to this day. In other sectors the advantages of this engine for power plant, ship propulsion and automobiles was also proposed (Chiras, 2002)

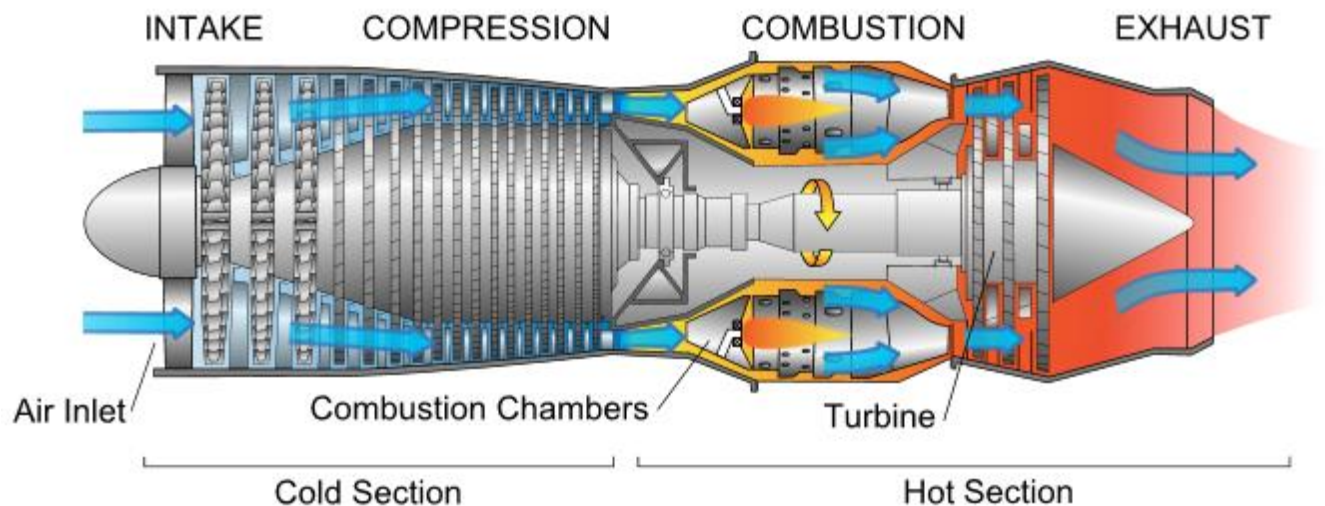


Figure 1.1: general gas turbine schematic (U.S. Department of Transportation Federal Aviation Administration, Airplane Flying Handbook, 2004)

A general gas turbine schematic includes three sections connected in series starting with the compressor then the combustion chamber and then the power turbine section. Gas turbine working principles are similar to the combustion engine where power is generated from a mixture of fuel and compressed air. As illustrated in figure 1.1 there are four processes in the gas turbine cycle. This commences with air flowing through the air inlet as a result of the low pressure inside the air intake caused by the compressor unit. Then the compressed air inside the compression section is mixed with fuel in the combustion chamber. The mixed air and fuel is then ignited causing expansion and the activation of the power turbine. This is how the gas turbine engine converts the energy stored in the fuel to produce mechanical work. (Meherwan P.Boyce., 2006)

In general the three processes stages of gas turbine includes: compression , combustion and expansion are referred to as the Brayton cycle. The gas turbine Brayton cycle was named after the American mechanical engineer George Brayton (1830- 1892). Figure (1.2) shows the ideal gas turbine Brayton Cycle. The actual cycle is different due to the turbulence and engine internal friction. (Meherwan P. Boyce, 2006)

A car gas turbine was tested by the Rover car company in 1950. This vehicle completed the Le Mans 24 hour race. A problem of gas turbine car engines is the sound which was unexpected to consumers. Gas turbine engines run at lower efficiency when operating on less than full load owing to incomplete combustion. (Phillips P. A. 2006)

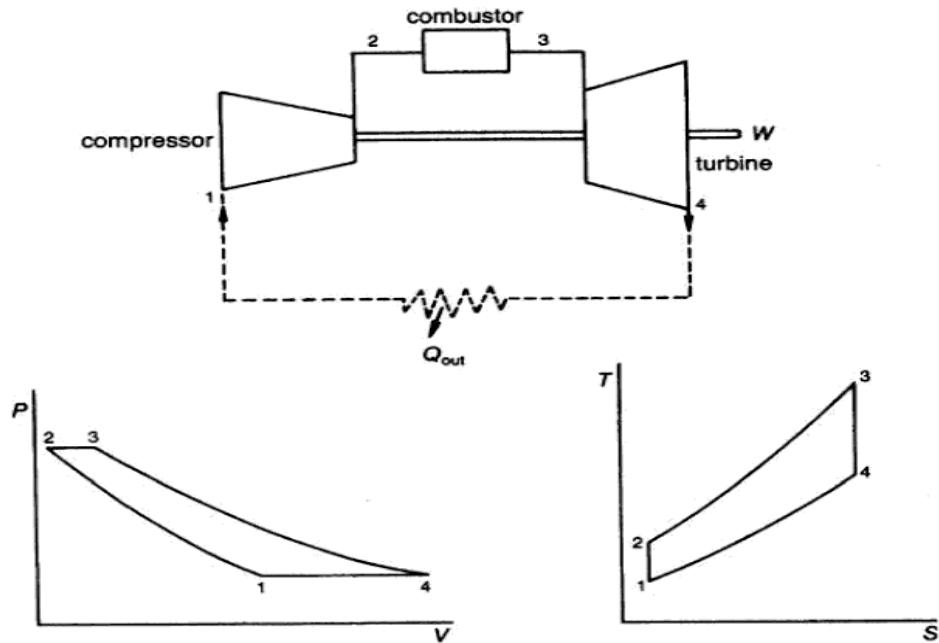


Figure 1.2: Brayton Cycle (Meherwan P. Boyce, 2006)

Nevertheless, the response characteristics of gas turbines on full load is as good as diesels. This and the power weight characteristics of gas turbines encouraged further research.

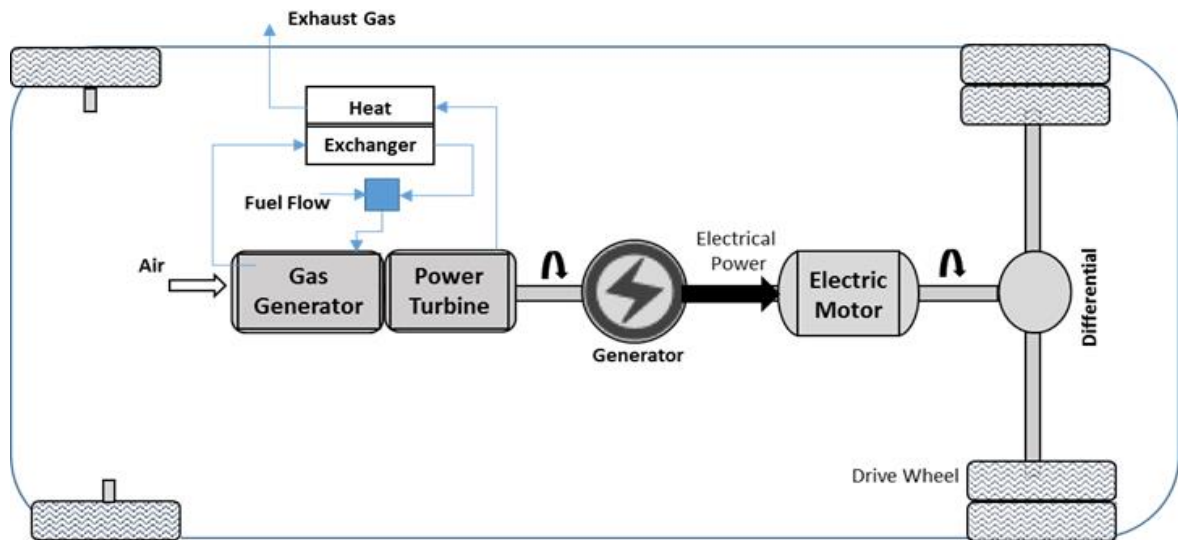


Figure 1.2: gas turbine with electric generator for electric drive vehicles

(E. Megdadi, R. Whalley and K. M. Ebrahimi, PMC2016, 2016)

Research into gas turbine electric drive systems, helps to reduce the gearing problems and high shaft rotating speed while reducing the exhaust gas temperature by providing an exhaust gas recovery cycle.

In this paper the gas turbines used for heavy duty, automotives which run over long distances will be considered.

1.2 Problem statement:

The regulation of automotive gas turbines will be investigated in this research study. using a multivariable system model. This represents the gas turbine with outputs of gas temperature (T) and the angular speed (ω) and, fuel flow ($f.f.$) and the nozzle area ($n.a.$) as inputs.

The research in this study aims to regulate the gas turbine angular speed (ω) by regulating the fuel flow ($f.f.$) and the nozzle area ($n.a.$). The rapid system response with lower output interaction and disturbance rejection behavior is required to obtain suitable, automotive system response characteristics.

Multivariable system models are more complicated than single input, single output systems models because of output interaction. Both outputs are affected by any system input change and this affects system stability. However, this research also deals with the control system energy consumption which affects maintenance cost, wear, heat and noise generation.

1.3 Aims and objectives:

A least effort controller will be used for regulation of the power turbine shaft speed and gas temperature, whilst obtaining acceptable changes in steady state via a closed loop strategy. The least effort controller, presented by Whalley R. and Ebrahimi M. (2004) solves the problems of stability, transient and steady state response with minimum output interaction.

In this research, a comparative study with an H infinity controller design will be produced. Comparing these controllers shows improvements in the speed response by decoupling the system outputs with least control energy consumption. The complexity of each control method, for purpose of implementation, will also be discussed.

1.4 Research Organization

Section one introduces a gas turbine history, operation and automotive engine applications. Then it gives the problem statement with the research aims and objectives.

Section two provides a literature survey regarding gas turbine control and a brief review of the control strategies used in this research together with control theory history and developments.

Section three discusses the gas turbine extended and reduced modeling with the gas turbine open loop response, including the controller requirements to achieve stability with well-behaved transients, and minimum settling time.

Section four discusses the control methods used in the comparative study and the equations and calculation required by each method.

Section five is concerned with the design steps for least effort and H infinity control, starting with the required equations, and design parameters.

Section six deals with the control system comparison and implementation. Results from the simulation using the MatLab programming language, simulation results and control objectives will be presented.

As a part of this research a comparative study will be conducted in section seven, highlighting the controller design and implementation difficulties of each technique, while focusing on the energy consumed by each method.

Finally, "Conclusions" and "Recommendations" are outlined in order to focus on each control method and recommendation for development and implementation purposes.

Section two:

Literature Review

2.1 Introduction

The earliest gas turbine regulation system used a manual operated hydraulic valve to manage the fuel required to achieve the desired, gas turbine power output. Figure 2.1 shows the diagram of a gas turbine basic control system starting from the power requested by the operator which is compared with the output to compute the fuel flow.

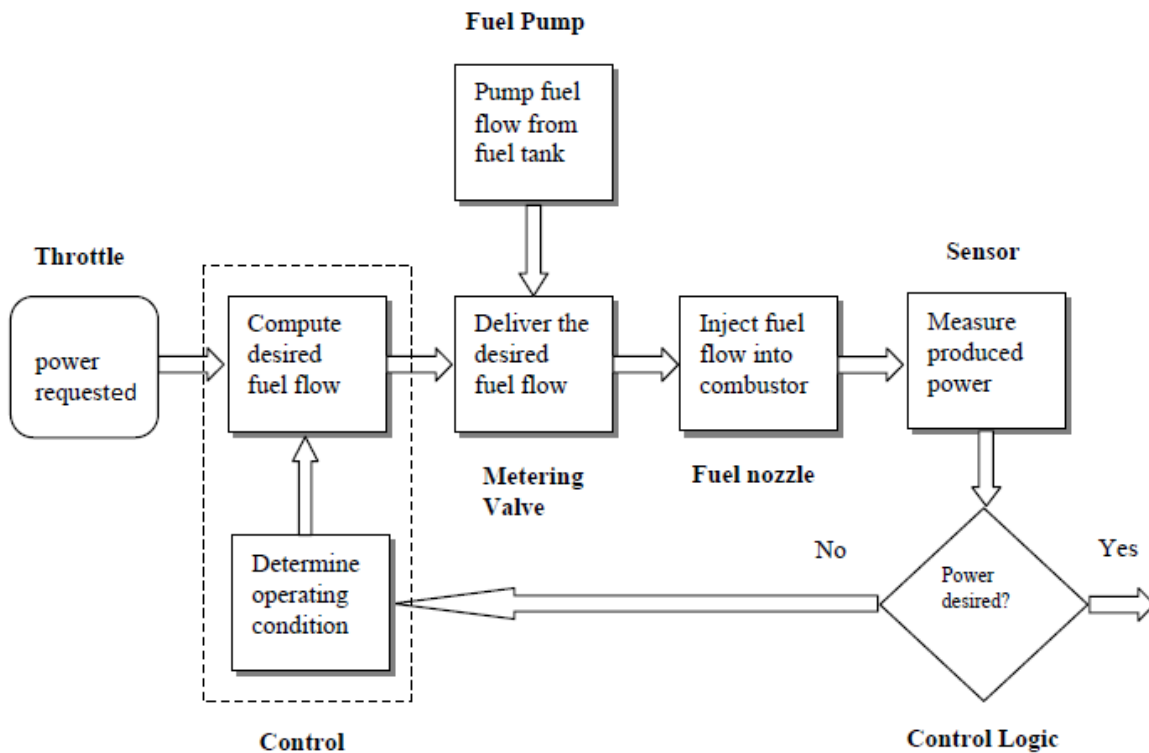


Figure 2.1 diagram of gas turbine basic control system

(Jaw & Garg, 2005)

Traditional control techniques such as stability and closed loop feedback will be used, by applying multivariable regulation principles. The least effort control method, will be compared with the H infinity method.

2.2 Control strategies review

Control theories have been implemented and investigated to solve the practical problems of regulation and system behavior. Engineers used the approach to understand the relationships between inputs and outputs, identifying the closed loop response, and the system stability. Feedback control strategies managed the system behavior by calculating the error or difference value between the actual output value of the system and the desired value, to achieve the output response and overall system stability.

Starting from water level regulating mechanism in tanks, in Greece in the period 300 to 1 B.C., this technique was used for water level processes. The industrial revolution period and mechanization development leading to automation technology and control theories are documented by (Dorf and Bishop, 2011).

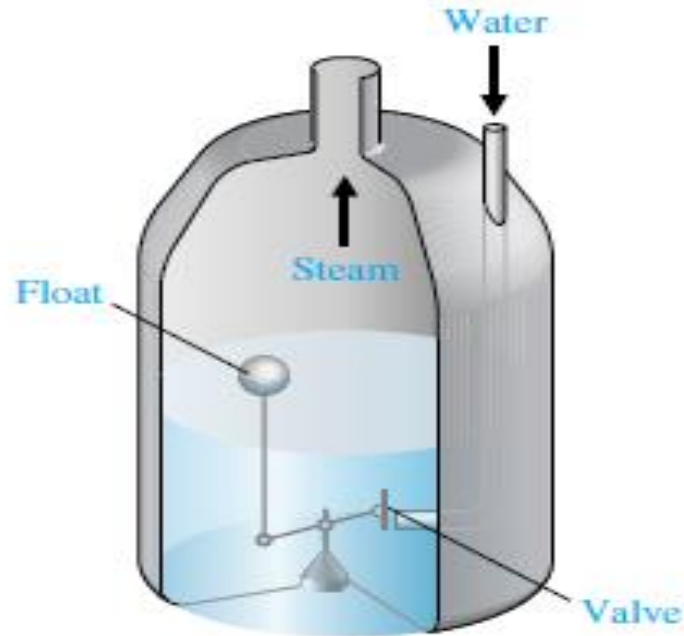


Figure 2.2: diagram of water level regulator system.

(Dorf and Bishop, 2011)

The temperature control system of Cornelis Drebbel (1572-133) appears to be the first control system used in Europe. Then the pressure control system in 1681 by Dennis Papin using a flyball governor was introduced. The governor was invented by James Watt's in 1769, to regulate a steam engine speed and was the first application of feedback control for industry. Figure (2.3) shows how the output shaft speed is measured and this changes the flyball movement in order to manage the amount of steam to the steam engine. As the output shaft rotates the flying ball movement causes the steam valve to close. (Otto Mayr, 1971).

Using floating ball, water level governor to control the water entering a boiler, was he first application of feedback by Plzunov in 1765. (Dorf and Bishop, 2011)

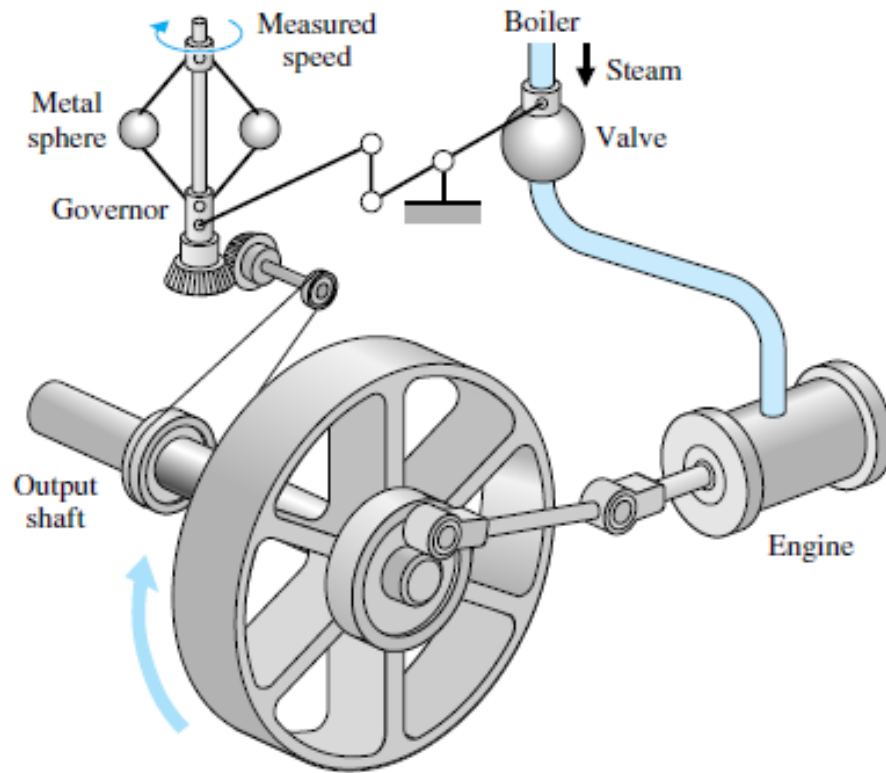


Figure 2.3 diagram of flyball governor system.

(Dorf and Bishop, 2011)

Using mathematical tools to represent actual systems started in the eighteenth century. Then differential equations were used to develop control system models. In world war II a huge improvement occurred in control theory because of the need to design control systems for radar, gun positioning, and other applications. Table 2.1 shows historical important developments of control science and applications, starting from the steam engine governor developed by James Watts, passing through to the developments of control systems such as the first formulation of system models for industry applications. Table (2.1) details the important development in control engineering.

1769	James Watt's steam engine and governor developed. The Watt steam engine is often used to mark the beginning of the Industrial Revolution in Great Britain. During the Industrial Revolution, great strides were made in the development of mechanization, a technology preceding automation.
1800	Eli Whitney's concept of interchangeable parts manufacturing demonstrated in the production of muskets. Whitney's development is often considered to be the beginning of mass production.
1868	J. C. Maxwell formulates a mathematical model for a governor control of a steam engine.
1913	Henry Ford's mechanized assembly machine introduced for automobile production.
1927	H. W. Bode analyzes feedback amplifiers.
1932	H. Nyquist develops a method for analyzing the stability of systems.
1952	Numerical control (NC) developed at Massachusetts Institute of Technology for control of machine-tool axes.
1954	George Devol develops "programmed article transfer," considered to be the first industrial robot design.
1960	First Unimate robot introduced, based on Devol's designs. Unimate installed in 1961 for tending die-casting machines.
1970	State-variable models and optimal control developed.
1980	Robust control system design widely studied.
1990	Export-oriented manufacturing companies emphasize automation.
1994	Feedback control widely used in automobiles. Reliable, robust systems demanded in manufacturing.
1997	First ever autonomous rover vehicle, known as Sojourner, explores the Martian surface.
1998–2003	Advances in micro- and nanotechnology. First intelligent micromachines are developed and functioning nanomachines are created.

Table 2.1: important developments of control science.

(Dorf and Bishop, 2011)

The developments of H infinity and least effort controller will be presented and discussed, as they are the chosen methods in this comparative study.

2.3 Classical control theory

Control science developed in three stages the first stage called the primitive stage of automotive control started in the end of 1860s to the beginning of 1900s. This is called Control science development stage 1900s. In 1960 the classical and the modern stage started through to the present day.

2.3.1 Open loop controller concept:

The concept of open loop control is based on managing the system output directly, without using feedback, therefore with open loop control it is not possible to maintain the relationship between variables by comparing these variables and improving thereby process system accuracy.

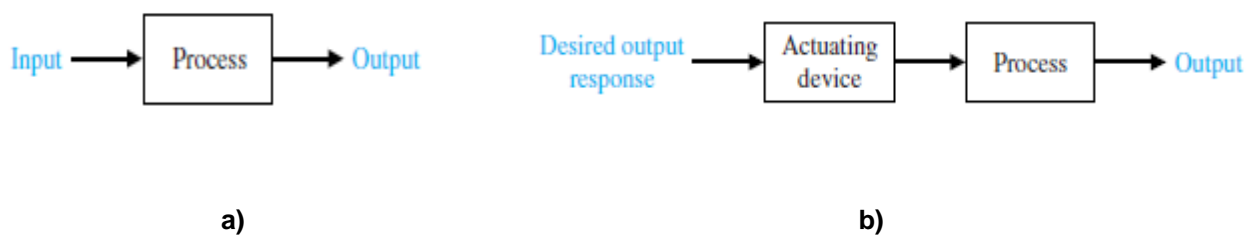


Figure 2.4: process of open loop controller:

a) System to be controlled. **b)** Open loop controller

(Dorf and Bishop, 2011)

2.3.2 Feedback controller concept:

“Feedback is a central feature of life. The process of feedback governs how we grow, respond to stress and challenge, and regulate factors such as body temperature, blood pressure and cholesterol level. The mechanisms operate at every level, from the interaction of proteins in cells to the interaction of organisms in complex ecologies.”

M. B. Hoagland and B. Dodson, *The Way Life works*, 1995 [99] - (Karl Johan Aström, Richard M. Murray, *Feedback Systems*, 2008)

Feedback concepts are based on the comparing the output variables with the desired values to obtain the system error.

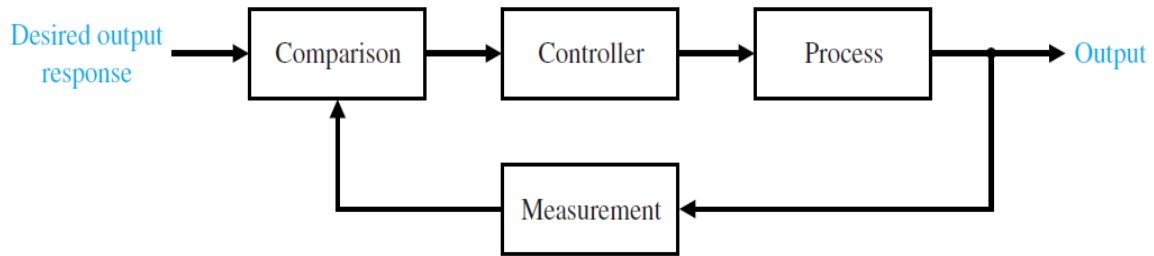


Figure 2.5: process of feedback controller
(Dorf and Bishop, 2011)

The comparison process starts by measuring the output value, then producing a feedback signal to compare it with the reference value, which represents the desired output.

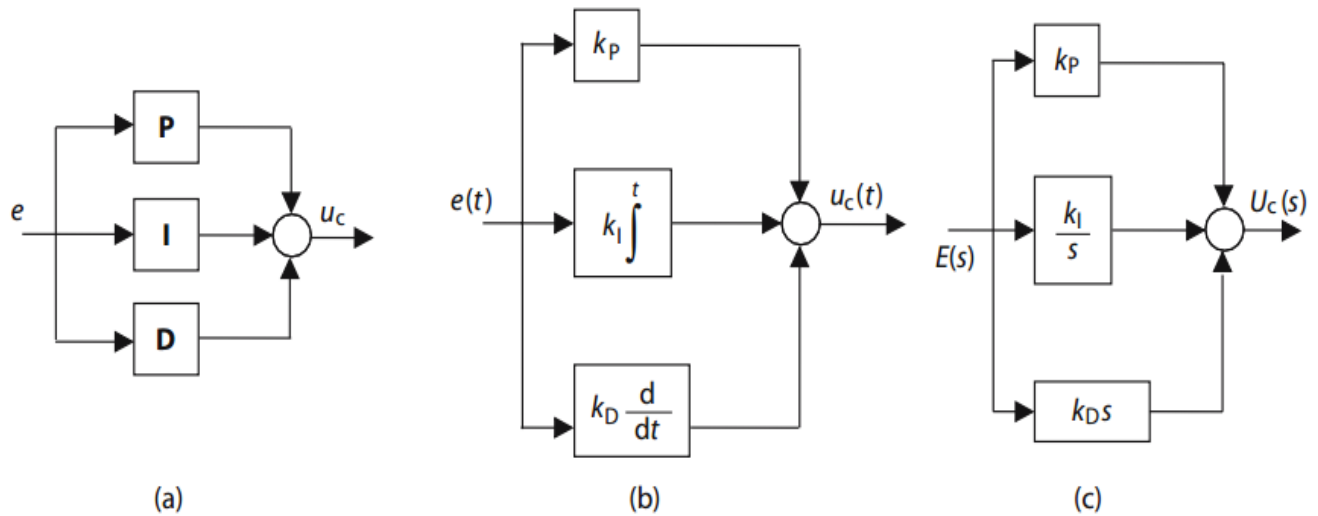
2.3.3 PID controller:

Proportional–integral–derivative (PID) controller is a control strategy that works by measuring the difference between the reference point and the actual system output. The system output follow the desired value using PID control represented by equation (2.1) using proportional, integral and derivative components:

$$\mathbf{u} = K_P \mathbf{e} + K_I \int \mathbf{e} + K_D \dot{\mathbf{e}} \quad \dots\dots\dots(2.1)$$

PID controller started to be used early in 1930s as a trial and error control approach by selecting K_P , K_I and K_D parameters. The aim of this approach is to obtain zero error in the output. While e representing the current output error, $\int e$ representing the accumulated integral output error. These basics allowed engineers to adjust and tune the controller to achieve the required output of the system. This is still a sufficient

method in many industry applications and still included in 95 percent of industrial control applications. (Edge 1997)



Key	Controller input e (system error)	PID control signal u_c			
Symbolic forms	e, u_c	Time domain forms	$e(t), u_c(t)$	Laplace domain forms	$E(s), U_c(s)$
Proportional gain	k_p	Integral gain	k_I	Derivative gain	k_D

Figure 2.6: PID controller representation
(Johnson M. A. & Moradi M. H., 2005)

Figure (2.6) shows a PID controller representation general as in (a) and the time domine form as in (b) and in laplace transform form as in (c).

2.3.4 Routh Hurwitz stability concept:

Representing physical models of actual systems as a polynomial, gives the ability to test a systems response by a mathematical strategy developed by the British scientist E. John Routh (1876). The polynomial is consider as stable if its roots are in the left half plane or in the unit disk. The famed Routh-Hurwitz stability criterion developed as a consequence of realizing the new Routh Hurwitz stability criterion started to be used in 1911. (Gopal, 2008)

Routh-Hurwitz stability concept dealing with the main issue in the controller design process by evaluating system stability and giving the system roots in the left half s-plane without calculating the exact values of these roots. This allows designers to choose a suitable method and control parameters that will produce a stable close loop system response.

2.4 The British control school

Many of British scientist, researchers and engineers, contributed and developed control theory and here are some of the methods and techniques developed by the British school.

2.4.1 Nyquist control theory

Nyquist stability theory was invented by H. Nyquist in 1932 at New Jersey Nokia Bell Labs, it is based on using the graph known as a Nyquist plot to obtain the system stability and there is no need to calculate the zeros and poles of the closed loop system. (H. Nyquist, 1932)

The inverse Nyquist control theory has been improved by the British engineer Rosenbrock (1969-1974) to include multi input multi output systems. In multivariable systems changing one input affects more than one output due to system input interaction, and this make it difficult of applying classical control methods. Using this approach to obtain a pre compensator reduce input interaction by changing diagonal dominance which make it possible to apply single input-output system control methods. (John O'Reilly, 1987)

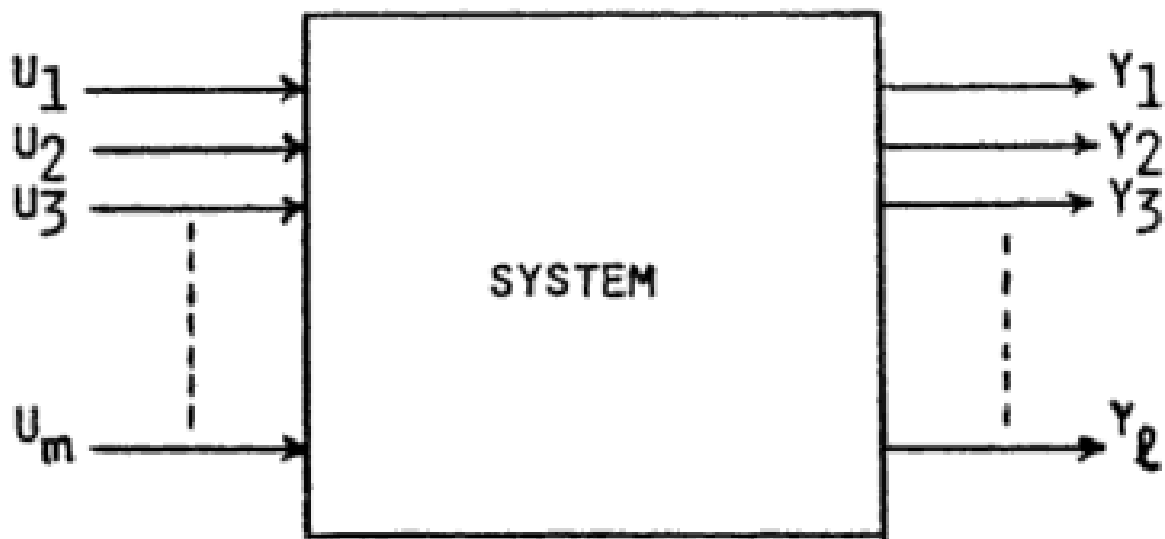


Figure 2.7: representation of a multivariable system

(John O'Reilly, 1987)

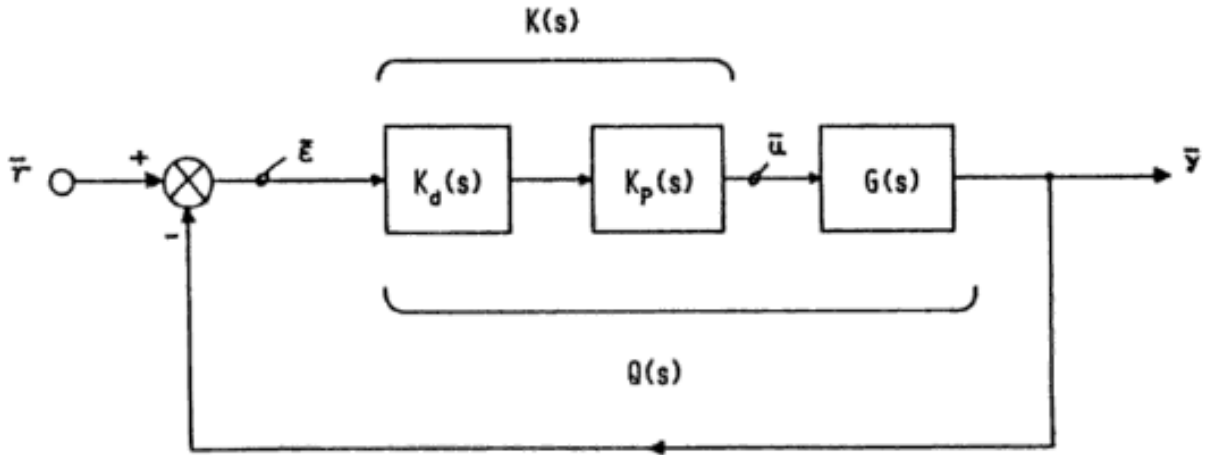


Figure 2.8: feedback regulating block diagram of multivariable system

(John O'Reilly, 1987)

Figure (2.8) shows that the regulating matrix $K(s)$ is the product of the multivariable pre compensator $K_p(s)$ and the diagonal tuning matrix $K_d(s)$.

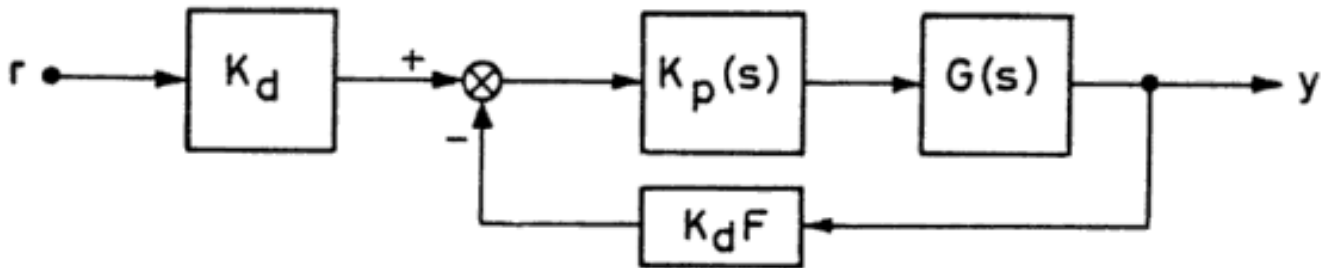


Figure 2.9: rearrangement of feedback regulating block diagram of multivariable system

(John O'Reilly, 1987)

Using rearrangement of feedback regulating block diagram of multivariable system of Figure (2.9) shows that the diagonal matrix F can be represented in the gain space. The closed loop transfer function is represented by the equation (2.2)

$$H(s) = (I + G(s)K(s)F) - 1 G(s)K(s) \quad \dots\dots\dots(2.2)$$

If the poles of H(s) in the left half s-plane then the control system is asymptotically stable. The main way to obtain the system stability in inverse Nyquist array is by using Gershgorin bands, which plot a group of disks contained the system eigenvalues with a calculated radius from the sum of the moduli of the off-diagonal elements. (John O'Reilly, 1987)

2.5 The American control school

Many American scientist, researchers and engineers also contributed and developed control theory. Here are some of the methods and techniques developed by the American school.

2.5.1 State space modeling

State space is one of the modern control methods which were firstly adopted by Leroy MacColl after studying Soviet researches and journals in the 1930s. Because Soviet researchers developed state space methods derived by Poincare and Lyapunov in the 19th century it was used by Kalman as a mathematical representation for control systems. (Kalman, 1960)

A state space model is obtained by relating system state variables, inputs and outputs using differential equations. Then representing state variables, input and output as vectors which allows control system using algebraic techniques, matrixes and vectors. This approach resulted in an effective way to analyze and solve multi-input and multi-output system models. These models use the least number possible of state variables reflecting thereby the order of a given system of differential equations.

The equations used to represent the state space at the same time show the system inputs, outputs and state variables as:

$$\dot{\mathbf{x}}(t) = \mathbf{A}(t)\mathbf{x}(t) + \mathbf{B}(t)\mathbf{u}(t)$$

$$\mathbf{y}(t) = \mathbf{C}(t)\mathbf{x}(t) + \mathbf{D}(t)\mathbf{u}(t)$$

where :

\mathbf{A} is the system state matrix

\mathbf{B} is the system input matrix

\mathbf{C} is the system output matrix

\mathbf{D} is the system forward feed matrix which is a zero matrix

\mathbf{x} is the system state vector

\mathbf{y} is the system output vector

\mathbf{u} is the system input vector

Figure (2.10) shows the representing block diagram of state space modeling.

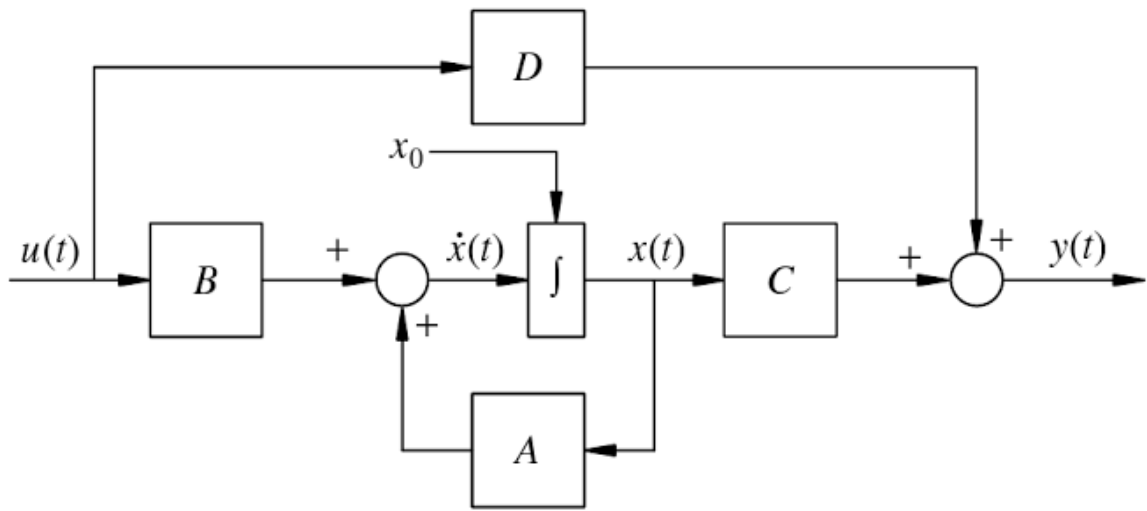


Figure 2.10: representing block diagram of state space modeling
(Robert L. Williams, II & Douglas A. Lawrence, 2007)

State space originated in control engineering science in the 1960s by Kalman R. E.. Then n the state space models were applied in control science to analyze and solve multi-input multi-output system models.

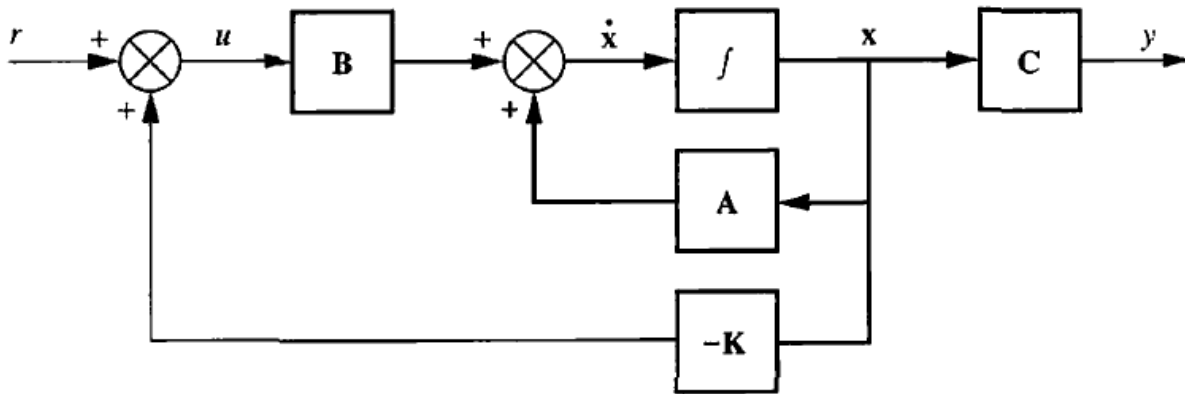


Figure 2.11: representing block diagram of state space modeling with feedback gain
(Norman S. Nise, 2006)

The usual control technique is the use of a negative feedback matrix K by setting $u(t) = Ky(t)$ in:

$$\dot{x}(t) = A(t)x(t) + B(t)Ky(t)$$

$$y(t) = C(t)x(t) + D(t)Ky(t)$$

Then the closed loop form becomes :

$$\dot{x}(t) = (A + BK(I - DK)^{-1}C)x(t)$$

$$y(T) = (I - DK)Cx(T)$$

Using the representing $(A + BK(I - DK)^{-1}C)$ to change the system Eigenvalues by choosing the suitable value of the gain matrix K

2.5.2 Optimal controller method

This control strategy uses a mathematical method developed in the beginning of 1950s by L. Pontryagin and R. Bellman, after studying applied mathematics researches. (Bryson, A. E., 1996)

An optimal controller method based on using a group of differential equations represent the control element paths which minimize a cost or loss function. The Optimal controller can be obtained using the partial differential equation of Hamilton–Jacobi–Bellman (HJB) equation. (Ross, I. M. ,2009).

The Optimal controller for linear quadratic representation minimized the following equation.

$$J = \int_0^{\infty} (\mathbf{x}(t)^T \mathbf{Q} \mathbf{x}(t) + \mathbf{u}(t)^T \mathbf{R} \mathbf{u}(t)) dt$$

Using the H constraint equation as the following:

$$H(\mathbf{x}, \mathbf{u}, \mathbf{p}, t) = \frac{1}{2} (\mathbf{x}^T \mathbf{Q} \mathbf{x} + \mathbf{u}^T \mathbf{R} \mathbf{u}) + \mathbf{P}^T (\mathbf{A} \mathbf{x} + \mathbf{B} \mathbf{u})$$

With the partial differential of H equaling zero the system input becomes:

$$\mathbf{u} = -\mathbf{R}^{-1} \mathbf{B}^T \mathbf{P}$$

All this results in the optimal gain of $\mathbf{R}^{-1} \mathbf{B}^T \mathbf{P}$ as shown in the following diagram:

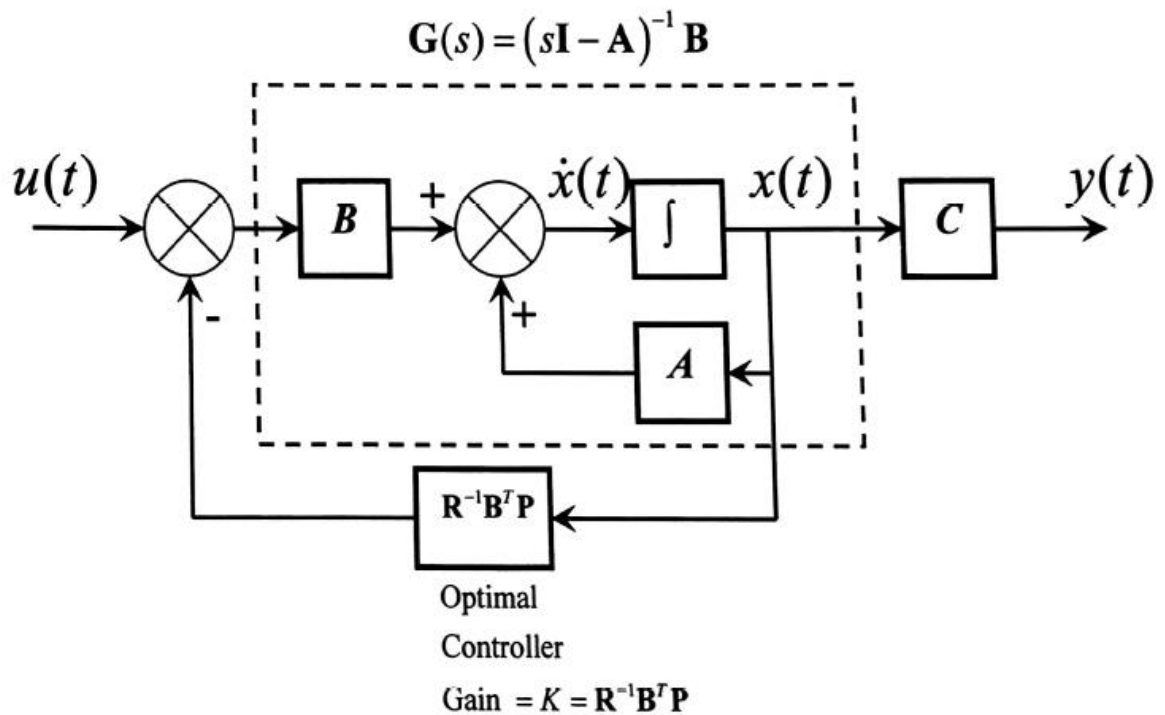


Figure 2.12: optimal controller feedback gain diagram.

(Whalley R., "lecture notes", 2015)

Using the steady state Riccati Equation this yields:

$$\mathbf{0} = \mathbf{A}^T \mathbf{P} + \mathbf{P} \mathbf{A} - \mathbf{P} \mathbf{B} \mathbf{R}^{-1} \mathbf{B}^T \mathbf{P} + \mathbf{Q} \quad \dots\dots\dots(2.3)$$

to select the **Q** and **R** matrix to obtain the **P** matrix and then select the appropriate gain.

2.6 Main issues and concepts of control theory:

2.6.1 Stability

Stability is the main issue in the controller designing process. In general a linear system is stable when it's bounded input values lead to a bounded output value. The marginal stable system is stable under some conditions and may be stable under other conditions because the system poles in the S-plan are on the complex axis.

2.6.2 Controllability and Observability

Controllability and Observability is a very important concept in the design stage because it indicates a suitable control method for the target system. Controllability shows the ability to obtain the desired system output using a suitable control input. Observability shows the ability to measure and observe system states and indicate if any of system states can be used to obtain the desired system output (Gilbert E. G., 1962)

2.6.3 Robust control

Robust theory is to obtain system stability with the existence of disturbances on the system. Robust theory started actively in the 1980s after the improved control methods of the American researcher Bode (1905- 1982) and others. Robust control was obtained

by multiple feedback and forward paths which allow high gain to be used to suppress system disturbances.

Robustness was achieved in many modern control methods such as the least effort controller and H infinity controller techniques.

2.7 The control methods used in this research:

2.7.1 Least effort controller review:

The least effort control strategy proposed by Whalley, R and M Ebrahimi (2006), is based on closed loop analysis procedures, which aim to minimize the control effort effect required for multivariable system regulation purposes. In so doing, actuator actively, wear, heat generation and noise are all minimized, with the employment of the low gain, passive feedback strategy invoked.

Least effort controller system achieves its design by using the minimum value of the system performance index (J). The technique in this method is based on analyzing an inner and outer loop. Low steady state, output interaction, following reference input changes can be achieved by this approach.

The design strategy to be adopted here will be to adjust the inner loop $k(s)$ and $h(s)$ vectors providing thereby “well behaved” dynamic conditions. Thereafter, with the pre-compensator P, configured to produce acceptable output coupling, and the outer loop feedback gain f becomes the final design parameter enabling the achievement of desired, dynamic and disturbance suppression characteristics.

2.7.2 H infinity controller review

H infinity control is used to achieve system robustness and dynamic performance . One of the designing methods for H infinity controller is H infinity loop shaping because the requested performance can be integrated in the design stage, as performance weights. This method with others was introduced by Zames G. in the early eighties which was suitable for multivariable system problems. (Ankit B.and Veena S. “Design and Analysis of Robust H-infinity Controller”)

H infinity controller is complicated because of the high order control algorithm required, the high controller energy required and the more difficulties in design and implementation. The controller $K(s)$ of H infinity technique should provide three criteria starting with stability, performance and robustness.

The stability of H infinity controller is ensured, when the characteristic equation roots, represented by equation (2.4), are in the left side of the s plane.

$$1 + G(s)K(s) = 0 \quad \dots\dots\dots(2.4)$$

The performance criterion achieved when the sensitivity represented by equation (2.5), has a small value for all frequencies. For robustness criterion the H infinity controller given to achieve high robustness for system performance:

$$S(s) = 1/(1 + G(s)K(s)) \quad \dots\dots\dots(2.5)$$

Section three

Research Methodology

3.1 Gas turbine modeling:

The gas turbine and electric power system shown in figure (3.1), with the system functions indicated represent and automotive gas turbine system. Two system outputs of gas temperature $T(s)$ and gas generator angular speed $w(s)$ are the two system outputs and fuel flow $f.f.(s)$ and nozzle area $n(s)$ are the inputs.

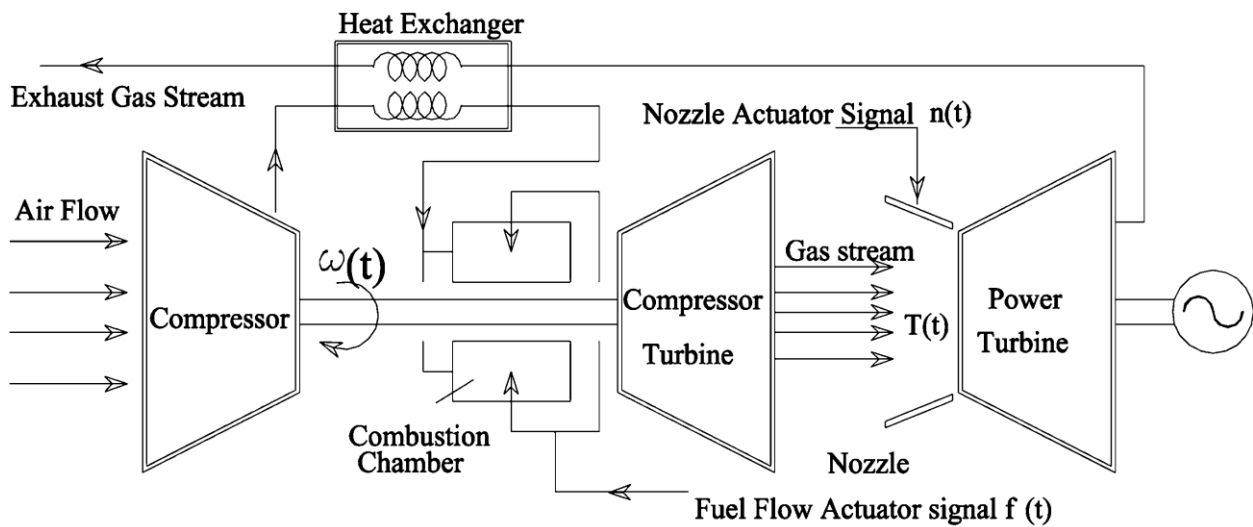


Figure 3.1: diagram of gas turbine connected electric power system
(E. Megdadi, R. Whalley and K. M. Ebrahimi, 2016)

The automotive gas turbine multivariable reduced system model can be represented by:

$$y(s) = G(s)u(s)$$

where the outputs are the changes in turbine speed and gas temperature, so that:

$$y(s) = \begin{bmatrix} T \\ \omega \end{bmatrix}$$

And the inputs are fuel pump and the guide vane angle changes, so that:

$$u(s) = \begin{bmatrix} f \cdot f \cdot \\ n \cdot a \cdot \end{bmatrix}$$

The automotive gas turbine model is represented in (3.1) where the matrix representing the system relations in the gas turbine is:

$$\bar{G}(s) = \begin{bmatrix} \frac{1.3(s + 258.46)10^6}{(s + 39.424)(s + 352.575)} & \frac{-5.6(s + 3.267)(s + 40.66)}{(s + 28.001)(s + 0.95)} \\ \frac{9.04(s + 31.42)10^6}{(s + 187.39)(s + 44.17)(s + 44.169)} & \frac{83.4(s + 75.5395)}{(s + 113.27)(s + 1.7214)} \end{bmatrix} \dots\dots\dots(3.1)$$

The reduced G(s) model is obtained by disregarding the remote poles and zeros. The final model is obtained by combining adjacent poles and maintaining steady state conditions. Then the system transfer function is:

$$G(s) = \begin{bmatrix} \frac{0.967 * 10^6}{s + 40.0} & \frac{-8.1248(s + 3.27)}{(s + 0.95)} \\ \frac{8.82 * 10^6(s + 31.42)}{(s + 1.55)(s + 40)(s + 187.4)} & \frac{50.20}{(s + 1.55)} \end{bmatrix} \dots\dots\dots(3.2)$$

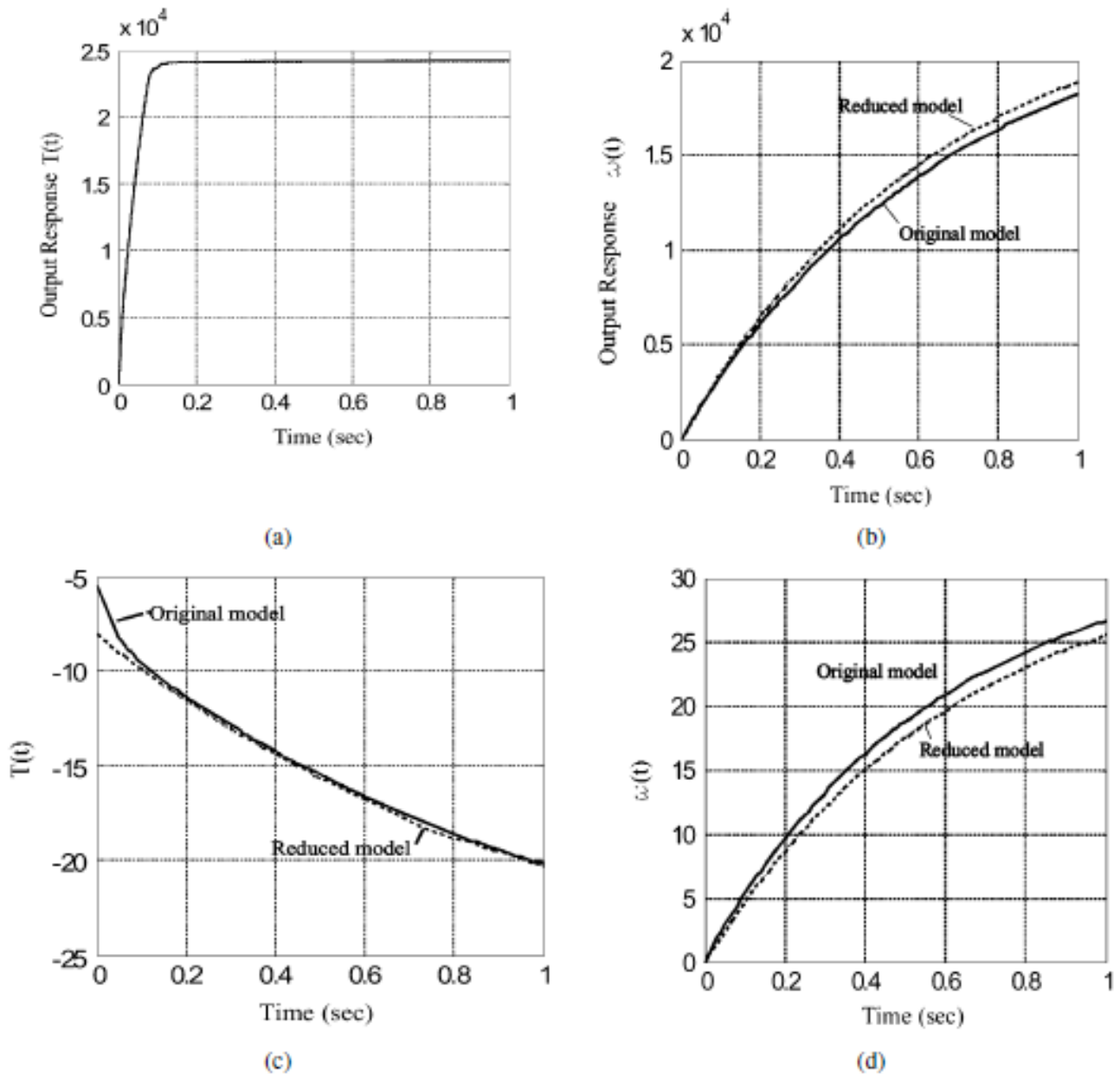


Figure 3.2: the actual gas turbine model with reduced transfer functions
(Whalley, R and Ebrahimi M, 2004)

Figure (3.2) shows that the reduced model is equivalent to the original model and can be used to investigate the system control.

3.2 Open loop response:

Using the reduced system transfer function $G(s)$ by applying a unit step change on system inputs figure (3.3) shows system outputs for 1 second after applying a 1% unity step change in Fuel Pump $\%f_p$. Figure (3.4) shows outputs response for one second after applying a 1% unity step change in the Guide Vane angle $\%n_a$. The Figures show an over damped response and relatively faster response in figure (3.3) than the response in figure (3.4). This response needs to be improved in terms of speed of reaction and output interaction.

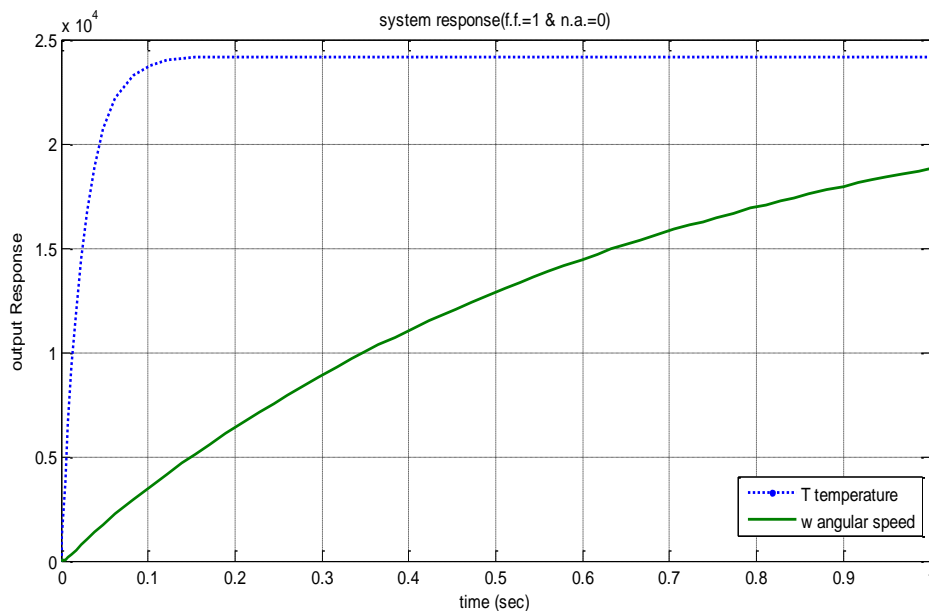


Figure 3.3: system response after applying a 1% unity step change in Fuel Pump $\% f_p$

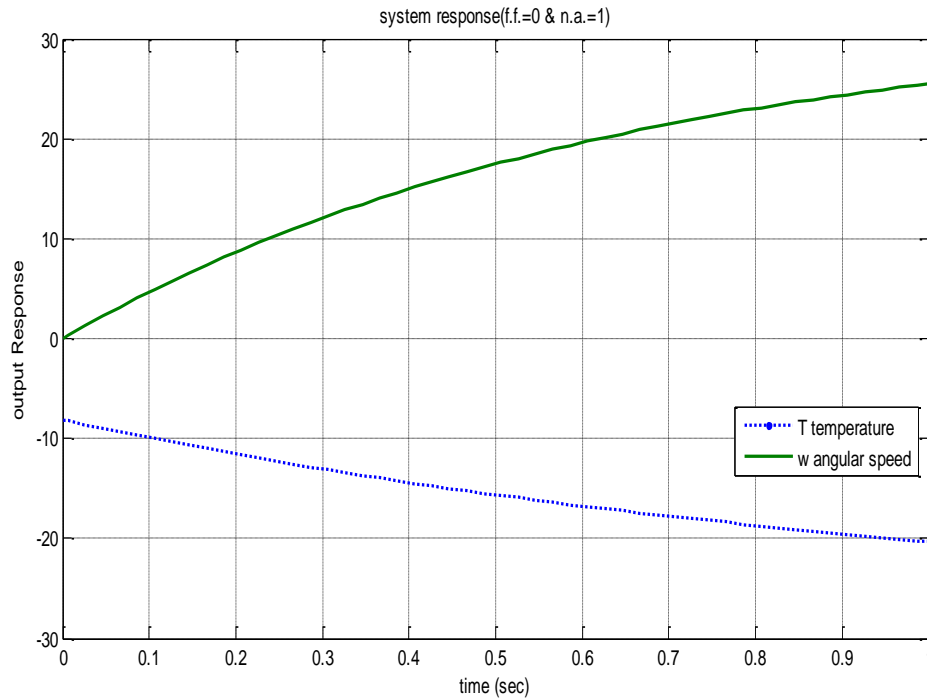


Figure 3.4: system response after applying a 1% unity step change in Guide Vane Unit % n_a

Each input affects both outputs, so the controller should reduce output coupling as much as possible. This should result, in changing any of the system inputs will change mainly one output with relatively small changes in the other output. The controller aims to achieve a stable well behaved response, with less than 20% overshoot, minimum settling time and rapid response. In this gas turbine model the controller should minimize the impact of random disturbances on system response with system's ability to rapidly recover from these disturbances.

This research investigation aims to achieve minimum effort control, with a simple controller design for easy implementation purposes.

3.3 Controller methods:

Least effort controllers control multivariable systems using an inner and outer loop. The function of the inner loop is to obtain acceptable transient conditions. The system outer loop function is to obtain the required steady state value and to ensure good disturbance rejection. The comparison with H infinity controller will illustrate the strengths and weaknesses of each strategy.

Section four:

Control theory

4.1 Least effort controller theory

4.1.1 Least effort controller technique:

In the least effort controller an inner loop is used to control the transient behavior of the system and outer loop to obtain the required steady state and to ensure disturbance suppression criteria.

The open loop system is represented by:

$$y(s) = G(s)u(s) + \delta(s) \quad \dots\dots\dots(4.1)$$

and closed loop control law given by:

$$u(s) = k(s)[\dot{r}(s) - h(s)y(s)] + P(r(s) - Fy(s)) \quad \dots\dots\dots(4.2)$$

The independent inputs in equations (4.1) and (4.22) they are m input and outputs and

$$F = \text{Diag}(f_1, f_2, \dots, f_m), 0 < f_j < 1, 1 \leq j \leq m \quad \dots\dots\dots(4.3)$$

The inner loop equation which used to obtain the transient performance is:

$$k(s)[\dot{r}(s) - h(s)y(s)] \quad \dots\dots\dots(4.4)$$

The outer loop equation which used to obtain the required steady state condition is:

$$P(r(s) - Fy(s)) \quad \dots\dots\dots(4.5)$$

With $\dot{r}(s) = 0$, the equation for the closed loop system becomes:

$$y(s) = (I_m + G(s)(k(s) \gg h(s) + PF))^{-1} \times (G(s) Pr(s) + \delta(s)) \quad \dots\dots\dots(4.6)$$

In terms of the steady state matrix S_s

$$y(0) = S_s r(0) \quad \dots\dots\dots(4.7)$$

Substituting $s = 0$ in equation(4.6)

$$P = (G(0)^{-1} + k(0) \gg h(0)S_s(I - FS_s)^{-1} \quad \dots\dots\dots(4.8)$$

To reduce the system output interaction, the steady state matrix should have unity diagonal elements and a small value, off-diagonal elements $S_{i,j}, 1 \leq i, j \leq m, i \neq j$.

Substituting for P from equation (4.8) equation (4.6) becomes:

$$y(s) = (I_m + G(s)(k(s) \gg h(s) + (G(0)^{-1} + k(s) \gg h(s)(I_m - F)^{-1}F))^{-1} \times (G(s) Pr(s) + \delta(s)) \quad \dots\dots\dots(4.9)$$

At low frequencies

$$G(s) \cong G(0) \text{ and } G(s)G(0)^{-1} \cong I_m$$

Substituting in equation (4.9):

$$y(s) = (I_m + G(s)(k(s) \gg h(s) + (I_m + (I_m - F)^{-1}F))^{-1} \times (G(s) Pr(s) + \delta(s)) \quad \dots \dots\dots(4.10)$$

Choosing the F matrix elements $f_1 = f_2 = \dots \dots f_m = f, 0 < f < 1$ then equation (4.10) becomes:

$$y(s) \cong (1 - f)(I_m + G(s)k(s) >< h(s))^{-1} \times (G(s) Pr(s) + \delta(s)) \quad \dots\dots\dots(4.11)$$

From equation (4.8) and (4.10):

$$G(s)P = G(s)(G(0)^{-1} + k(0) >< h(0))(I_m - F)^{-1}$$

This equation can be reduced for low frequencies to:

$$G(s)P \cong \frac{1}{1-f} (I_m + G(s)k(0) >< h(0)) \quad \dots\dots\dots(4.12)$$

Under steady state condition equation (4.12) is represented by:

$$y(s) = I_m r(s) + S(s)\delta(s) \quad \dots\dots\dots(4.13)$$

The equation for the sensitivity matrix at low frequencies is:

$$S(s) = (1 - f)(I_m + G(s)k(s) >< h(s))^{-1}, 0 < f < 1 \quad \dots\dots\dots(4.14)$$

When S_s is equal to I_m then the system has no interaction at steady state, giving enhanced stability and disturbance rejection at steady state with higher value of f , $f < 1$

Using a conventional regulator structure with forward path gain of $K(s)$ and a feedback gain $H(s)$ the closed loop equation is:

$$y(s) = (I_m + G(s)K(s)H(s))^{-1}(GK(s)r(s) + \delta(s)) \quad \dots\dots\dots(4.15)$$

Let $K(s) = P$. From equation (4.6) and (4.15):

$$K(s)H(s) = k(s) >< h(s) + PF \quad \dots\dots\dots(4.16)$$

$$H(s) = P^{-1}k(s) >< h(s) + F \quad \dots\dots\dots(4.17)$$

4.1.2 Inner loop calculations:

For an $m \times m$ system transfer function $G(s)$ the general equation is:

$$\mathbf{G}(s) = \mathbf{L}(s) \frac{A(s)}{d(s)} \mathbf{R}(s) \mathbf{\Gamma}(s) \quad \dots\dots\dots(4.18)$$

Where elements of $L(s), A(s), R(s), \Gamma(s)$ and $\frac{A(s)}{d(s)} \in H_\infty, s \in \mathbb{C}$

In equation () $L(s)$ for left row factors and $R(s)$ for right column factors of $G(s)$ and $\Gamma(s)$ for the transformed system time delays.

$$L(s) = \text{Diag} \left(\frac{\lambda_i(s)}{p_j(s)} \right), R(s) = \text{Diag} \left(\frac{\rho_i(s)}{q_i(s)} \right) \text{ and } \Gamma(s) = \text{Diag}(e^{-sT_j}), 1 \leq i, j \leq m$$

where $A(s) \neq 0$, and $a_{ij}s^{m-1} + b_{ij}s^{m-2} + \dots + \gamma_{ij}, 1 \leq i, j \leq m$

the inner loop equation for the system is:

$$\mathbf{u}(s) = \mathbf{k}(s)[\dot{\mathbf{r}}(s) - \mathbf{h}(s)\mathbf{y}(s)] \quad \dots\dots\dots(4.19)$$

From combining equations (4.1) and (4.19) yields:

$$\mathbf{y}(s) = (\mathbf{I}_m + \mathbf{G}(s)\mathbf{k}(s) \mathbf{h}(s))^{-1} (\mathbf{G}(s)\mathbf{k}(s)\dot{\mathbf{r}}(s) + \boldsymbol{\delta}(s)) \quad \dots\dots\dots(4.20)$$

The $k(s)$ equation becomes:

$$\mathbf{k}(s) = (\mathbf{k}_1(s)e^{-s(T_i-T_j)}, \mathbf{k}_2(s)e^{-s(T_i-T_j)}, \dots, \mathbf{k}_m(s)e^{-s(T_i-T_j)})^T \quad \dots\dots\dots(4.21)$$

and $\mathbf{h}(s) = (\mathbf{h}_1(s), \mathbf{h}_2(s), \dots, \mathbf{h}_m(s))$

Since $\phi_j(s)$ and $x_j(s)$ are stable, minimum phase, strictly proper or proper functions then $k_j(s) = k_j(s)\phi_j(s)$ and $h_j(s) = h_jx_j(s)$ for $1 \leq j \leq m$ then $y(s)$ becomes:

$$y(s) = \left(I_m + e^{-sT} n(s)L(s) \frac{A(s)}{d(s)} k(s) \right) \left(n(s)L(s) \frac{A(s)}{d(s)} k e^{-sT} r(s) + \delta(s) \right) \dots\dots\dots(4.22)$$

With: $k = (k_1, k_2, \dots, k_m)^T$, $h = (h_1, h_2, \dots, h_m)$, $d(s) = s^k, a_1s^{k-1} + \dots + a_0$

and $\deg(n(s)a_{i,j}(s)) < k$, for $1 \leq i, 1 \leq m$.

The determinant of equation (4.22) is:

$$\det \left(I_m + e^{-sT} n(s)L(s) \frac{A(s)}{d(s)} k(s) \right) = 1 + e^{-sT} n(s) \left\langle h \frac{A(s)}{d(s)} k \right\rangle$$

where $\left\langle h \frac{A(s)}{d(s)} k \right\rangle = [1, s, \dots, s^{m-1}] \begin{bmatrix} \gamma_{11} & \gamma_{12} & \dots & \gamma_{1m} \\ \vdots & \vdots & \ddots & \vdots \\ b_{11} & b_{12} & \dots & b_{1m} \\ a_{11} & a_{12} & \dots & a_{1m} \end{bmatrix} \begin{bmatrix} k_1 h_1 \\ k_2 h_1 \\ \vdots \\ k_m h_m \end{bmatrix}$

with gain ratio of:

$$k_2 = nk_1, k_3 = n_2k_1, \dots, k_m = n_{m-1}k_1$$

and $\left\langle hA(s)k \right\rangle = b(s)$, $k_1[Q]h = (b_{m-1}, b_{m-2}, \dots, b_0)^T$

$$Q = \begin{bmatrix} \gamma_{11} + \gamma_{12}n_1 + \gamma_{1m}n_{m-1} & \vdots & \gamma_{21} + \gamma_{22}n_1 + \gamma_{2m}n_{m-1} & \vdots & \gamma_{m1} + \gamma_{m2}n_1 + \gamma_{mm}n_{m-1} \\ \vdots & \vdots & \vdots & \vdots & \vdots \\ b_{11} + b_{12}n_1 + b_{1m}n_{m-1} & \vdots & b_{21} + b_{22}n_1 + b_{2m}n_{m-1} & \vdots & b_{m1} + b_{m2}n_1 + b_{mm}n_{m-1} \\ a_{11} + a_{12}n_1 + a_{1m}n_{m-1} & \vdots & a_{21} + a_{22}n_1 + a_{2m}n_{m-1} & \vdots & a_{m1} + a_{m2}n_1 + a_{mm}n_{m-1} \end{bmatrix}$$

Selecting n values so the Q matrix is invertible. the performance index becomes:

$$J = (1 + n_1^2 + n_2^2 + \dots + n_{m-1}^2)b^T(Q^{-1})^TQ^{-1}b \quad \dots\dots\dots(4.23)$$

Should be minimized by selecting the $b(s)$ and the gain ratio n , so the closed loop dynamics can be obtained and the h vector can be calculated where $k_1 \neq 0$.

4.2 H infinity controller theory

H-infinity controller technique is widely used for the control problems including multivariable systems. The controller resulting is optimal with the respect that the resulting function does not necessarily represent the best controller solution.

In the H-infinity control technique the general feedback structure shown in figure (4.1) is used

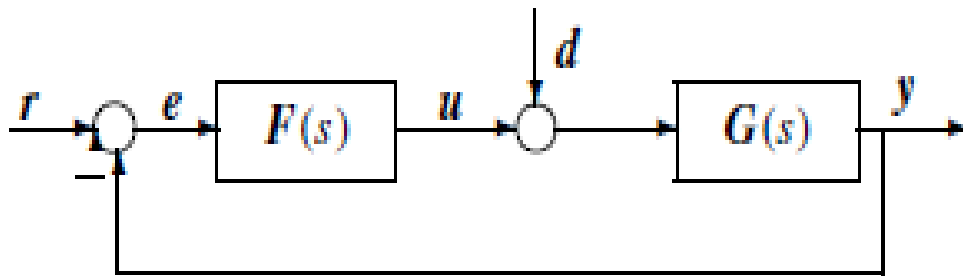


Figure 4.1: Feedback control structure typical (Dingyu X, YangQuan C and Derek P, 2007)

The matrix representing the H-infinity controller is:

$$\mathbf{F}_c = \begin{bmatrix} \mathbf{A}_f & \vdots & -\mathbf{ZL} \\ \dots & \dots & \dots \\ \mathbf{F} & \vdots & \mathbf{0} \end{bmatrix}$$

Where:

$$\mathbf{A}_f = \mathbf{A} + \gamma^{-2} \mathbf{B}_1 \mathbf{B}_1^T \mathbf{X} + \mathbf{B}_2 \mathbf{F} + \mathbf{Z} \mathbf{L} \mathbf{C}_2, \mathbf{F} = -\mathbf{B}_2^T \mathbf{X} \quad \text{and} \quad \mathbf{L} = -\mathbf{Y} \mathbf{C}_2^T, \mathbf{Z} = (\mathbf{I} - \gamma^{-2} \mathbf{Y} \mathbf{X})^{-1}$$

For the robust control the following structure is used in general:

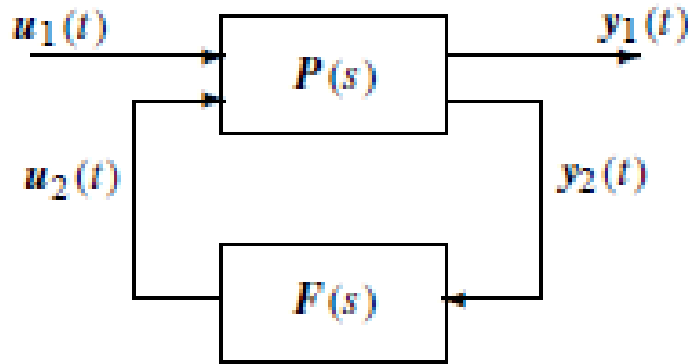


Figure 4.2 : general structure of feedback control
(Dingyu X, YangQuan C and Derek P, 2007)

The following representing the system plant model.

$$\begin{bmatrix} s\dot{\mathbf{x}}(s) \\ \mathbf{y}_1(s) \\ \mathbf{y}_2(s) \end{bmatrix} = \mathbf{P}(s) \begin{bmatrix} \mathbf{x}(s) \\ \mathbf{u}_1(s) \\ \mathbf{u}_2(s) \end{bmatrix} \quad \dots\dots\dots(4.1)$$

where the states, outputs and inputs of (4.1) equation are representing by $\mathbf{x}(s)$, $\mathbf{u}(s)$ and $\mathbf{y}(s)$, respectively, and $\mathbf{P}(s)$ as :

$$\mathbf{P}(s) = \begin{bmatrix} \mathbf{A} & \mathbf{B}_1 & \mathbf{B}_2 \\ \mathbf{C}_1 & \mathbf{D}_{11} & \mathbf{D}_{12} \\ \mathbf{C}_2 & \mathbf{D}_{21} & \mathbf{D}_{22} \end{bmatrix}$$

The equation representing the state space given by the following:

$$s\mathbf{x}(s) = \mathbf{A}\mathbf{x}(s) + [\mathbf{B}_1 \quad \mathbf{B}_2] \begin{bmatrix} \mathbf{u}_1(s) \\ \mathbf{u}_2(s) \end{bmatrix}$$

and for the system output equation:

$$\begin{bmatrix} y_1(s) \\ y_2(s) \end{bmatrix} = \begin{bmatrix} C_1 \\ C_2 \end{bmatrix} x(s) + \begin{bmatrix} D_{11} & D_{12} \\ D_{21} & D_{22} \end{bmatrix} \begin{bmatrix} u_1(s) \\ u_2(s) \end{bmatrix}$$

The equation showing the relation between $y_1(s)$ and $u_1(s)$ is:

$$\mathbf{T}_{y_1 u_1}(s) = \mathbf{P}_{11}(s) + \mathbf{P}_{12}(s)[\mathbf{I} - \mathbf{F}(s)\mathbf{P}_{22}(s)]^{-1}\mathbf{F}(s)\mathbf{P}_{21}(s)$$

where for the standard robust \mathcal{H}_∞ control problems:

$$\|\mathbf{T}(s)_{y_1 u_1}\|_\infty < 1$$

For optimal \mathcal{H}_∞ control problems, the $\min_{\mathbf{F}(s)} \|\mathbf{T}(s)_{y_1 u_1}\|_\infty$ to be selected as in the example given in [3]:

The weighting functions $W_1(s)$, $W_2(s)$ and $W_3(s)$, which representing the system filters, are to be selected, as per figure (4.3).

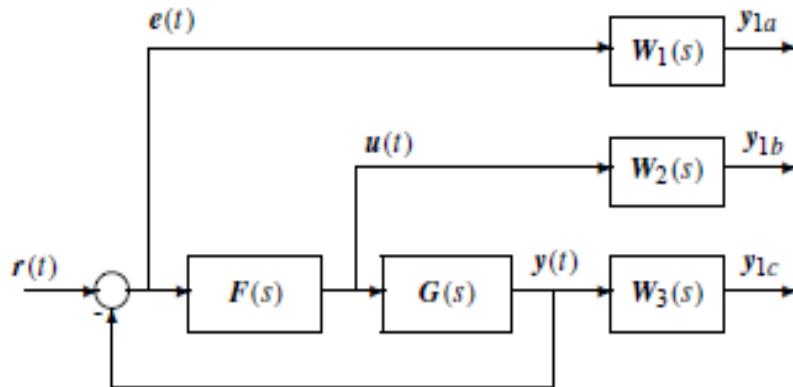


Figure4.3: structure of feedback control problem with weighting functions
(Dingyu X, YangQuan C and Derek P, 2007)

The relationship between the plant model and the plant weighting functions can be represented by the following matrix:

$$P(s) = \begin{bmatrix} W_1(s) & \vdots & -W_1(s)G(s) \\ \mathbf{0} & \vdots & W_2(s) \\ \mathbf{0} & \vdots & W_3(s)G(s) \\ \dots & \vdots & \dots \\ \mathbf{I} & \vdots & -G(s) \end{bmatrix}$$

where:

$$T_{y1u1} = \begin{bmatrix} W_1(s)S(s) \\ W_2(s)F(s)S(s) \\ W_3(s)T(s) \end{bmatrix}$$

where $F(s)$ is obtained from the sensitivity function $S(s)$:

$$S(s) = [I + F(s)G(s)]^{-1}$$

Then the complementary transfer function of sensitivity is:

$$T(s) = I - S(s) = F(s)G(s)[I + F(s)G(s)]^{-1}$$

Section five:

Controller Design

5.1 Design of the least effort controller

System transfer function is:

$$G(s) = \begin{bmatrix} \frac{0.967 * 10^6}{s + 40.0} & \frac{-8.1248(s + 3.27)}{(s + 0.95)} \\ \frac{8.82 * 10^6(s + 31.42)}{(s + 1.55)(s + 40)(s + 187.4)} & \frac{50.20}{(s + 1.55)} \end{bmatrix}$$

Using the form:

$$G(s) = L(s) \frac{A(s)}{d(s)} R(s) \Gamma(s) \quad \dots\dots\dots(5.1)$$

With the following left row factors, right column factors and transformed system time delays.

$$L(s) = \begin{bmatrix} \frac{1}{(s + 0.95)} & 0 \\ 0 & \frac{1}{(s + 1.55)(s + 187.4)} \end{bmatrix}$$

$$A(s) = \begin{bmatrix} 0.967(s + 0.95) * 10^6 & -8.1248(s + 3.27) \\ 8.82(s + 31.42)10^6 & 50.20(s + 187.4) \end{bmatrix}$$

$$R(s) = \begin{bmatrix} \frac{1}{(s + 40)} & 0 \\ 0 & 1 \end{bmatrix}$$

$$d(s) = (s + 1.55)(s + 400)(s + 187.4)$$

If:

$$\mathbf{k}(s) = \begin{bmatrix} \frac{s + 40.0}{s + 400.0} & 0 \\ 0 & \frac{1}{s + 400.0} \end{bmatrix} \begin{bmatrix} \mathbf{k}_1 \\ \mathbf{k}_2 \end{bmatrix}$$

and:

$$\mathbf{h}(s) = [\mathbf{h}_1, \mathbf{h}_2] \begin{bmatrix} \frac{s + 0.95}{(s + 1.55)(s + 187.4)} & 0 \\ 0 & 1 \end{bmatrix}$$

Then the following equation can be used to calculate the inner loop parameters:

$$\mathbf{y}(s) = (\mathbf{I}_m + \mathbf{G}(s)\mathbf{k}(s) \gg \mathbf{h}(s))^{-1} \mathbf{G}(s)\mathbf{k}(s)\dot{\mathbf{r}}(s) \quad \dots\dots\dots(5.2)$$

and the inner loop equation becomes:

$$\det(\mathbf{I}_m + \mathbf{G}(s)\mathbf{k}(s) \gg \mathbf{h}(s)) = 1 + \langle \mathbf{h}(s)\mathbf{G}(s)\mathbf{k}(s) \rangle \quad \dots\dots\dots(5.3)$$

Then equation (5.2) becomes:

$$-1 = \frac{b(s)}{(s + 1.55)(s + 400)(s + 187.4)} \quad \dots\dots\dots(5.4)$$

Figure (5.1) shows the root locus of the equation (5.4) to obtain the gain b_0

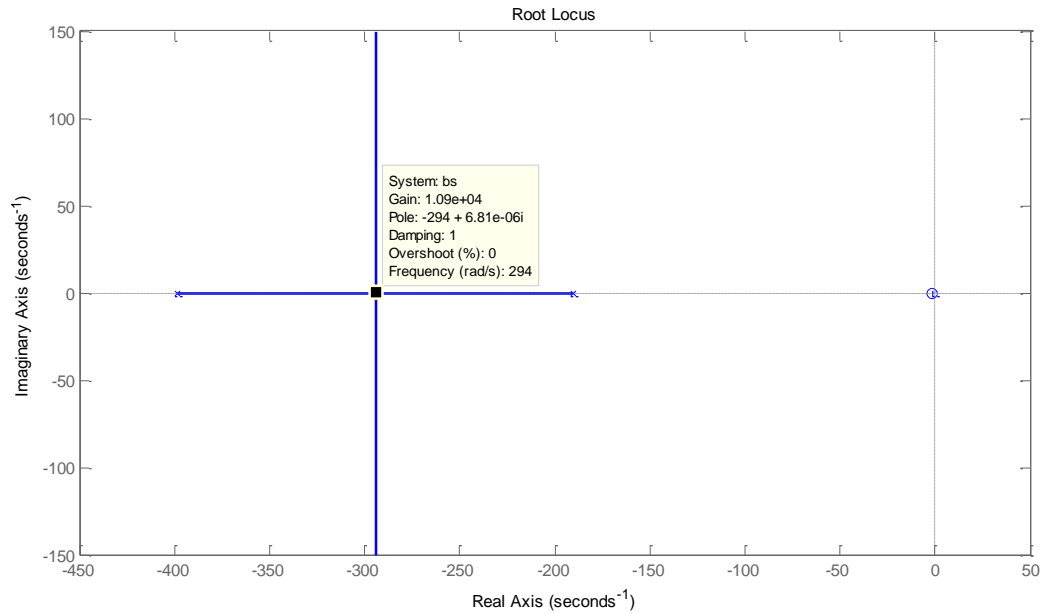


Figure 5.1: root locus of the equation (5.4)

To select the zeros of the equation $b(s) = b_0(s + 1.55)$ to achieve the required pattern for the system closed loop poles. From the root locus graph b_0 is (0 to $1.09 \cdot 10^4$), from the gain range $b_0 = 1.09 \cdot 10^4$ to be chosen for the closed loop poles at $-294 \pm 6.81 \cdot 10^{-6}i$

Calculating $\langle h.A(s).k \rangle = b(s)$ as following:

$$\langle h.A(s).k \rangle = [h_1 \ h_2] \cdot \begin{bmatrix} 0.967(s + 0.95) \cdot 10^6 & -8.1248(s + 3.27) \\ 8.82(s + 31.42)10^6 & 50.20(s + 187.4) \end{bmatrix} \cdot \begin{bmatrix} k_1 \\ k_2 \end{bmatrix}$$

$$\langle h.A(s).k \rangle = \begin{bmatrix} 0.967(s + 0.95) \cdot 10^6 \cdot h_1 + 8.82(s + 31.42)10^6 \cdot h_2 \\ -8.1248(s + 3.27) \cdot h_1 + 50.20(s + 187.4) \cdot h_2 \end{bmatrix}^T \cdot \begin{bmatrix} k_1 \\ k_2 \end{bmatrix}$$

$$\langle h.A(s).k \rangle = (0.967(s + 0.95) \cdot 10^6 \cdot h_1 + 8.82(s + 31.42)10^6 \cdot h_2) \cdot k_1 + (-8.1248(s + 3.27) \cdot h_1 + 50.20(s + 187.4) \cdot h_2) \cdot k_2$$

$$\langle \mathbf{h} \cdot \mathbf{A}(s) \cdot \mathbf{k} \rangle = [1 \quad s] \begin{bmatrix} 0.95 * 10^6 & -26.568 & 277.1244 * 10^6 & 9407.48 \\ 0.967 * 10^6 & -8.1248 & 8.82 * 10^6 & 50.20 \end{bmatrix} \cdot \begin{bmatrix} k_1 h_1 \\ k_2 h_1 \\ k_1 h_2 \\ k_2 h_2 \end{bmatrix}$$

.....(5.5)

Let $k_2 = n \cdot k_1$ and selecting then selecting $k_1 = 1$:

$$\langle \mathbf{h} \cdot \mathbf{A}(s) \cdot \mathbf{k} \rangle = [1 \quad s] \begin{bmatrix} 0.95 * 10^6 & -26.568 & 277.1244 * 10^6 & 9407.48 \\ 0.967 * 10^6 & -8.1248 & 8.82 * 10^6 & 50.20 \end{bmatrix} \times \begin{bmatrix} h_1 \\ n \cdot h_1 \\ h_2 \\ n \cdot h_2 \end{bmatrix}$$

$$\langle \mathbf{h} \cdot \mathbf{A}(s) \cdot \mathbf{k} \rangle$$

$$= [0.967(s + 0.95)10^6 \quad 8.82(s + 31.42)10^6 \quad -8.1248(s + 3.27) \quad 50.20(s + 187.4)]$$

$$\times \begin{bmatrix} h_1 \\ n \cdot h_1 \\ h_2 \\ n \cdot h_2 \end{bmatrix}$$

$$\langle \mathbf{h} \cdot \mathbf{A}(s) \cdot \mathbf{k} \rangle$$

$$= [0.95 * 10^6 + 0.967 * 10^6 s \quad -26.568 - 8.1248 s \quad 277.1244 * 10^6 + 8.82 * 10^6 s \quad 9407.48 + 50.20 s]$$

$$\times \begin{bmatrix} h_1 \\ n \cdot h_1 \\ h_2 \\ n \cdot h_2 \end{bmatrix}$$

Equation (5.5) can be represented as:

$$\langle \mathbf{hA}(s)\mathbf{k} \rangle = \mathbf{Q}(n)(\mathbf{h}_1, \mathbf{h}_2)^T$$

The Q matrix obtained as following:

$$Q = \begin{bmatrix} 0.95 * 10^6 - 26.568n & 277.1244 * 10^6 + 9407.48n \\ 0.967 * 10^6 - 8.1248n & 8.82 * 10^6 + 50.20n \end{bmatrix}$$

From equation (5.5) and equation (5.4):

$$\langle h \cdot \frac{A(s)}{d(s)} \cdot k \rangle = \frac{b(s)}{d(s)}$$

$$b(s) = b_0(s + x)$$

$$x = 1.55$$

Using vector [1 1.55] to remove the pole (s+1.55) , from the root locus of the following:

$$1 + \frac{b_0(s + 1.55)}{(s + 1.55)(s + 400)(s + 187.4)}$$

To calculate k_2 from the performance index J

$$J = (1 + n^2)b^T(Q^{-1})^T Q^{-1}b$$

Plotting performance index (J) with the system gain ratio using MATLAB, the numerical computing program. Then obtaining the n , producing the minimum value of performance index (J) using MATLAB code which occurs when:

$$\partial J(n)/\partial n = 0$$

Substituting $Q(n)$ and b

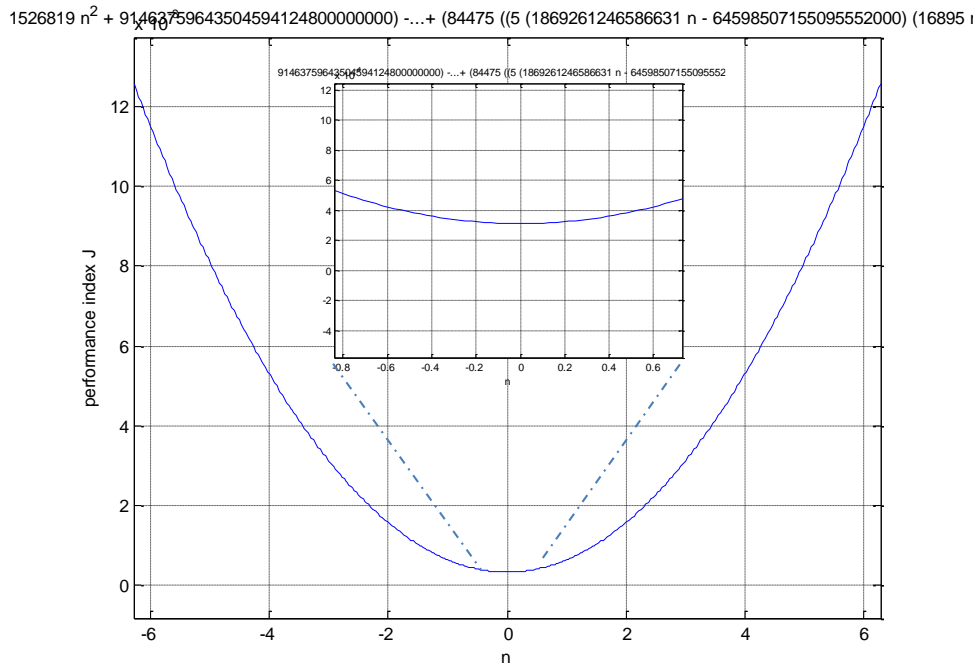


Figure 5.2: performance index with the gain ratio graph

With $(n = -7.4741 \cdot 10^{-6})$ performance index (J) has the lowest value of 0.0000089147422

Substitute n value in Q

$$Q = \begin{bmatrix} 9.1800e + 05 & 2.7720e + 08 \\ 9.6700e + 05 & 8.8200e + 06 \end{bmatrix}$$

Selecting $k_1 = 1$ and substituting in equation (5.6)

$$h(s) = \frac{Q^{-1}}{k_1} b \quad \dots\dots\dots(5.6)$$

$$h = \begin{bmatrix} 1.7646 * 10^{-2} \\ -1.9116 * 10^{-5} \end{bmatrix}$$

Using $k_2 = nk_1$ to obtain k as following:

$$k = \begin{bmatrix} 1 \\ -7.47416067 * 10^{-6} \end{bmatrix}$$

Outer loop design

For the Outer loop design it is required to find the P matrix of equation (4.8) is determined:

The steady state system transfer function at $s = 0$ is:

$$G(0) = \begin{bmatrix} 24175 & -27.9664 \\ 23851.3788 & 32.387 \end{bmatrix}$$

Using steady state inter action of 0.01 as following:

$$S_s = \begin{bmatrix} 1 & 0.01 \\ 0.01 & 1 \end{bmatrix}$$

Using outer loop feedback gain (f) from $f = 0.1$ to $f = 0.9$

Choosing $f = 0.95$

$$F = \begin{bmatrix} 0.95 & 0 \\ 0 & 0.95 \end{bmatrix}$$

Using the equation (4.8) to calculate P compensator:

$$P = \left(G(0)^{-1} + K(0) \gg h(0) \right) * S_s * (I - F * S_s)^{-1}$$

$$P = \begin{bmatrix} 6.2572e - 02 & 1.2678e - 02 \\ -2.7277e - 01 & 2.7833e - 01 \end{bmatrix}$$

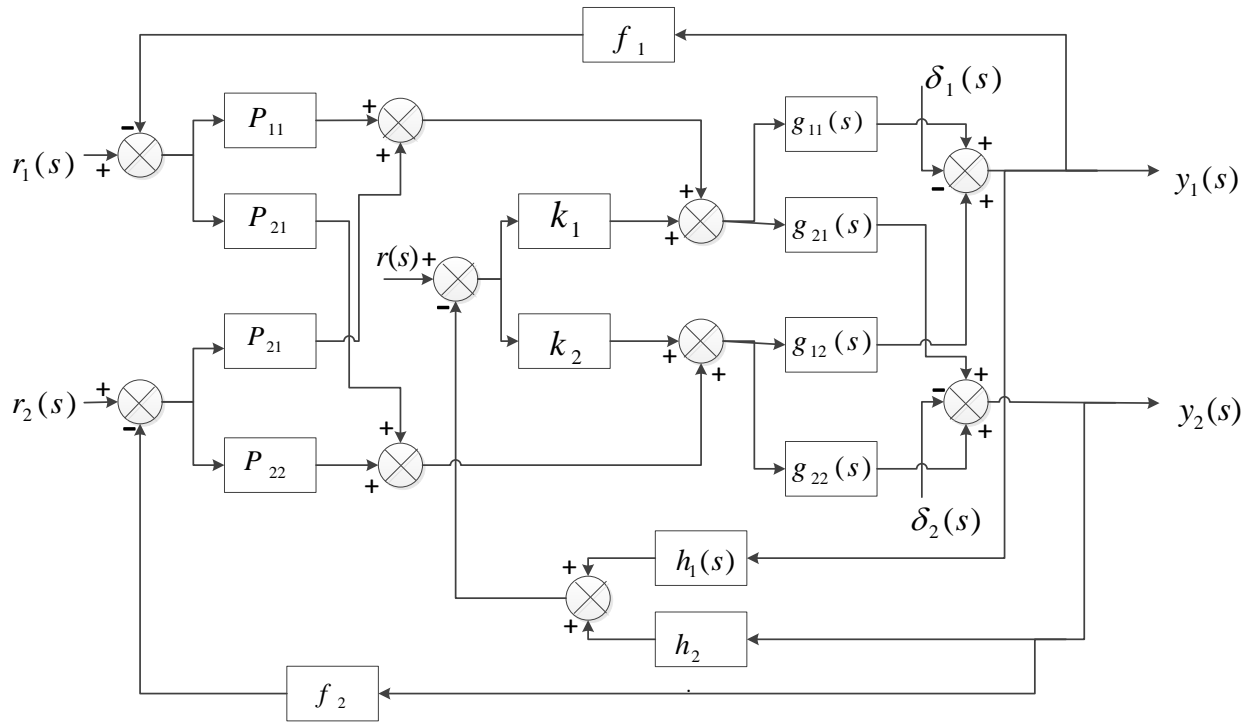


Figure 5.3: closed loop system representation

The conventional controller structure

H compensator is required to complete the conventional structure with the P matrix calculated in the previous section.

Using the following equation to calculate H compensator:

$$H = P^{-1} * K(0) >> h(0) + F$$

$$H = \begin{bmatrix} 9.8981e - 01 & -1.3184e - 04 \\ 3.9015e - 02 & 9.4987e - 01 \end{bmatrix}$$

With $r(s) = 0$ and using the following controller construction:

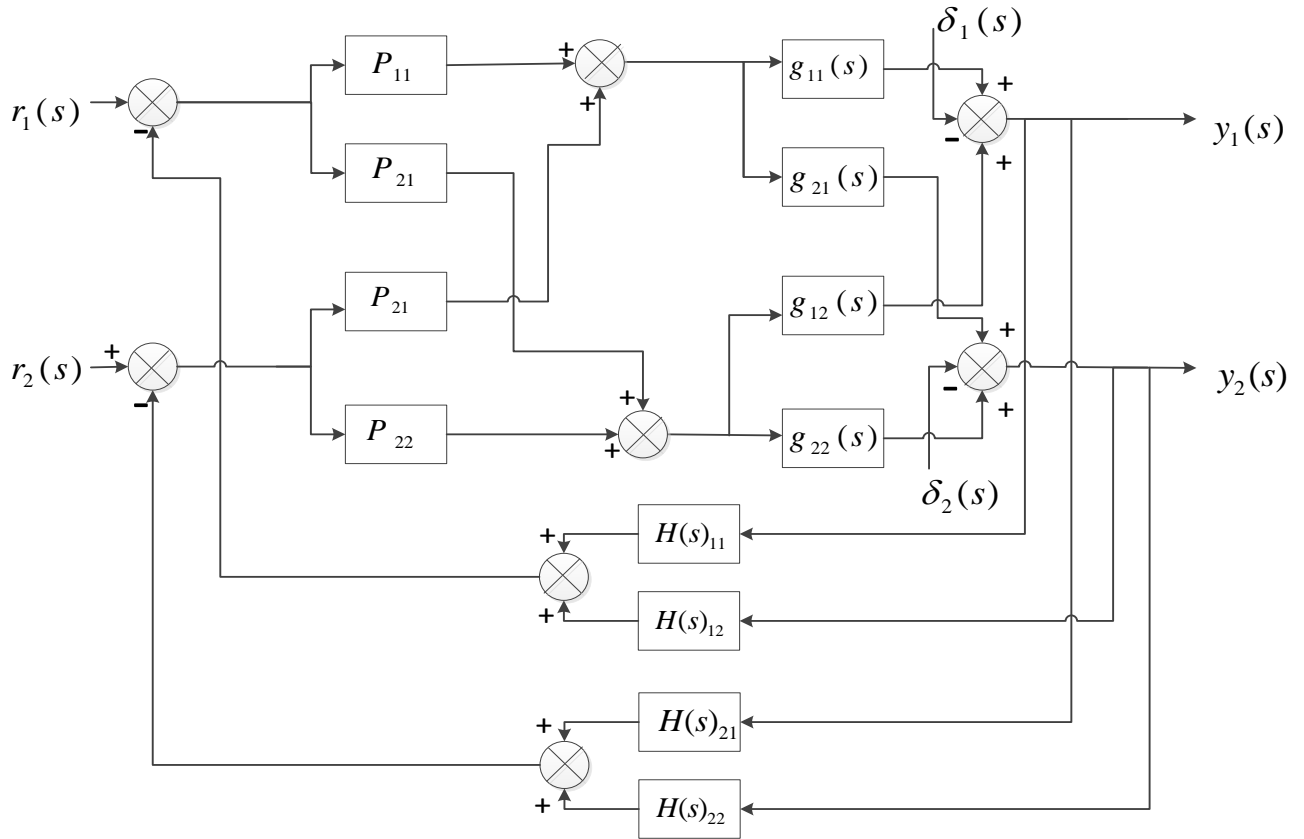


Figure 5.4: conventional closed loop system representation

5.2 H infinity controller design

By selecting the weighting function matrices for the system model which should be proper or in other words bounded when s goes to infinity (Dingyu Xue; YangQuan Chen & Deek P. Atherton, 2007) as following:

$$\mathbf{W}_1(s) = \begin{bmatrix} \frac{100}{s + 0.5} & 0 \\ 0 & \frac{100}{s + 1} \end{bmatrix}$$

$$\mathbf{W}_2(s) = \begin{bmatrix} 10^{-5} & 0 \\ 0 & 10^{-5} \end{bmatrix}$$

This values of $W_2(s)$ cancel any problems of singularity and avoid the determinant becomes zero. The weighting functions are chosen to be rational, stable, minimum phase functions with no RH plane poles. (John e. Bibel & D. Stephen Malyevac, 1992)

And:

$$W_3(s) = \begin{bmatrix} \frac{s}{1000} & 0 \\ 0 & \frac{s}{200} \end{bmatrix}$$

Referring to [3] (Dingyu X, YangQuan C and Derek P, 2007) and by using the MatLab application “augtf” function to get the variable γ of the system transfer function, and the MatLab function “hinftol” to get the minimum value of γ as follows:

```

<< H-Infinity Optimal Control Synthesis >>

```

No	Gamma	D11<=1	P-Exist	P>=0	S-Exist	S>=0	lam(PS)<1	C.L.
1	1.0000e+00	OK	OK	FAIL	OK	OK	OK	UNST
2	5.0000e-01	OK	OK	OK	OK	OK	OK	STAB
3	7.5000e-01	OK	OK	OK	OK	OK	OK	STAB
4	8.7500e-01	OK	OK	FAIL	OK	OK	OK	UNST
5	8.1250e-01	OK	OK	FAIL	OK	OK	OK	UNST
6	7.8125e-01	OK	OK	FAIL	OK	OK	OK	UNST
7	7.6563e-01	OK	OK	OK	OK	OK	OK	STAB
8	7.7344e-01	OK	OK	OK	OK	OK	OK	STAB
9	7.7734e-01	OK	OK	OK	OK	OK	OK	STAB

Iteration no. 9 is your best answer under the tolerance: 0.0100 .

Table 5.1: the results obtain from MatLab application for the synthesis of H-infinity optimal controller.

By selection $\gamma = 7.7734 \times 10^{-1}$, then $F_c(s)$ is:

$$\mathbf{F}_c(s) = \begin{bmatrix} \mathbf{F}_{11}(s) & \mathbf{F}_{12}(s) \\ \mathbf{F}_{21}(s) & \mathbf{F}_{22}(s) \end{bmatrix}$$

Where:

$$\mathbf{F}_{11}(s)$$

$$= \frac{1.6826 (s + 3259) (s + 187.4) (s + 40)^2 (s + 1.55) (s + 1) (s + 0.9439)}{(s + 2.14e04) (s + 253.9) (s + 84.55) (s + 40) (s + 1.55) (s + 1.396) (s + 1) (s + 0.5)}$$

$$\mathbf{F}_{12}(s)$$

$$= \frac{21.449 (s + 187.4) (s + 40)^2 (s - 14.98) (s + 1.55) (s + 0.8405) (s + 0.5)}{(s + 2.14e04) (s + 253.9) (s + 84.55) (s + 40) (s + 1.55) (s + 1.396) (s + 1) (s + 0.5)}$$

$$\mathbf{F}_{21}(s)$$

$$= \frac{245.87 (s - 2.534e04) (s + 245.2) (s + 40) (s + 20.69) (s + 1.55) (s + 1) (s + 0.95)}{(s + 2.14e04) (s + 253.9) (s + 84.55) (s + 40) (s + 1.55) (s + 1.396) (s + 1) (s + 0.5)}$$

$$\mathbf{F}_{22}(s)$$

$$= \frac{8217 (s + 405.2) (s + 206.6) (s + 40) (s + 4.784) (s + 1.55) (s + 0.95) (s + 0.5)}{(s + 2.14e04) (s + 253.9) (s + 84.55) (s + 40) (s + 1.55) (s + 1.396) (s + 1) (s + 0.5)}$$

$F_c(s)$ is the controller obtained from H-infinity method. And \mathbf{F}_{21} , \mathbf{F}_{21} , \mathbf{F}_{21} and \mathbf{F}_{21} are the controller matrix elements

The controller matrix element \mathbf{F}_{21} shows a non-minimum phase algorithm. The effect of this non-minimum phase algorithm will be discussed in the "Comparison Study" section.

Section six:

Simulation

6.1 Least effort controller simulation:

The analytical structure of the closed loop system is shown in figure (5.3). The second reference $r_2(s)$ is used to achieve the required acceleration. The first reference will be constant value reflecting the gas temperature limit of the power turbine. So a single input will be required for vehicle operation.

By using a unit step at the first system reference $r_1(s)$ and then on the second reference $r_2(s)$ for the closed loop system response. This response is shown in figures (6.1) and (6.2) gives least interaction between the outputs with a fast system response.

figures (6.1) and (6.2) shows that the system response for angular speed output with different f values with the output reaching its steady state value after 0.25 sec., for an outer loop feedback gain of $f = 0.95$.

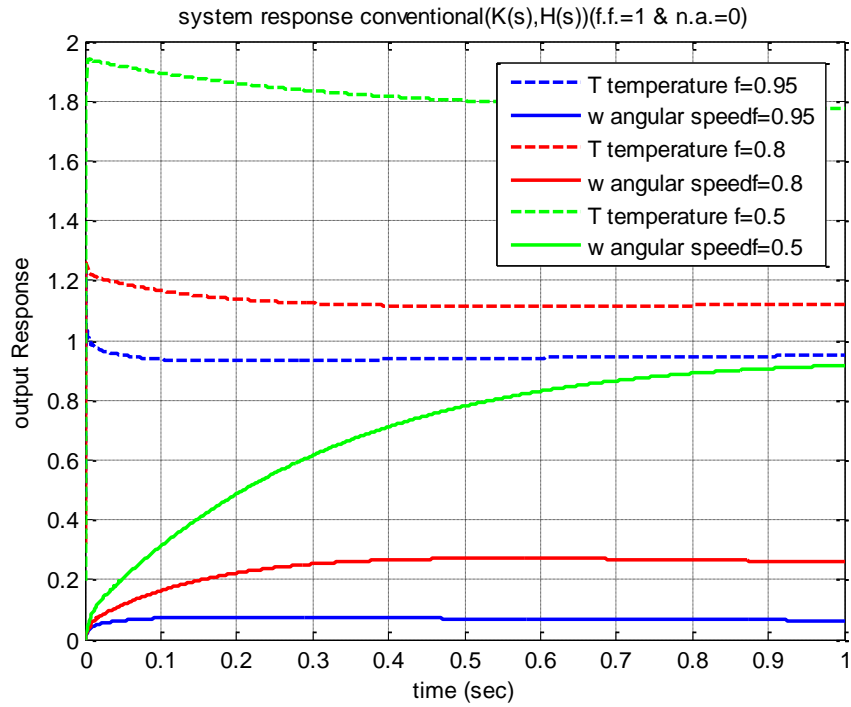


Figure 6.1: System response after applying a unit step change at $r_1(s)$

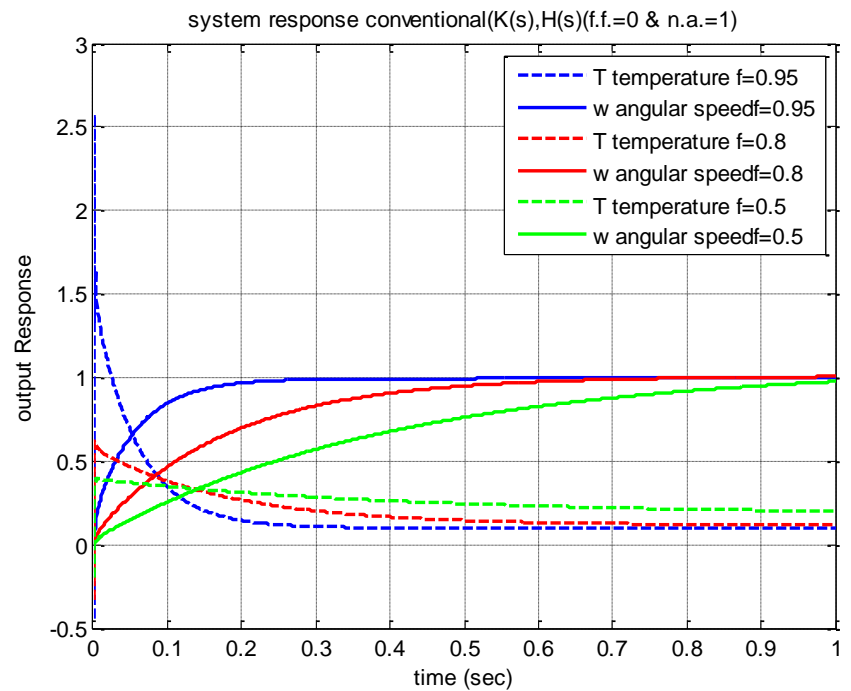


Figure 6.2: System response after applying a unit step change at $r_2(s)$

Figures (6.1) and (6.2) show the improvement in the angular speed output of system, with the system response becoming faster for increasing f values

A unit step input at $\delta_1(s)$ and $\delta_2(s)$ is used to show the system response following disturbances. Figures (6.3) and (6.4) show system's ability to suppress disturbances. Results show that the system with least effort controller has a high disturbance rejection performance.

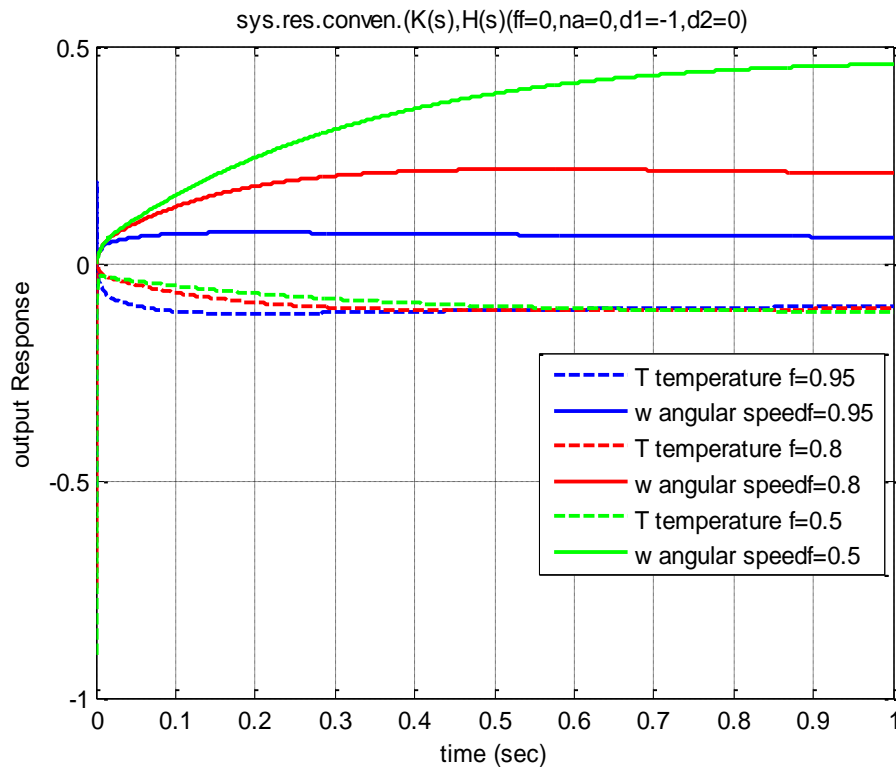


Figure 6.3: System response after applying a negative unit step at $\delta_1(s)$

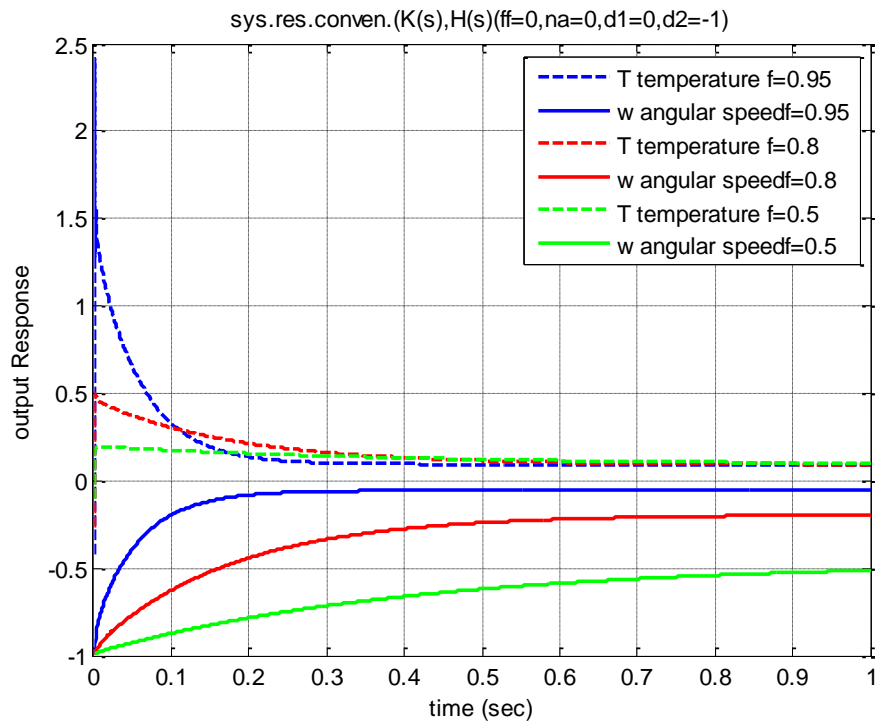


Figure 6.4: System response after applying a negative unit step at $\delta_2(s)$

6.2 H-infinity controller simulation:

Using a unit step as the first system reference $r_1(s)$ and then on the second reference $r_2(s)$ for the closed loop system response. The response shown in figures (6.5) and (6.6) is very fast, but with high output interaction when applying the input on the second reference $r_2(s)$.

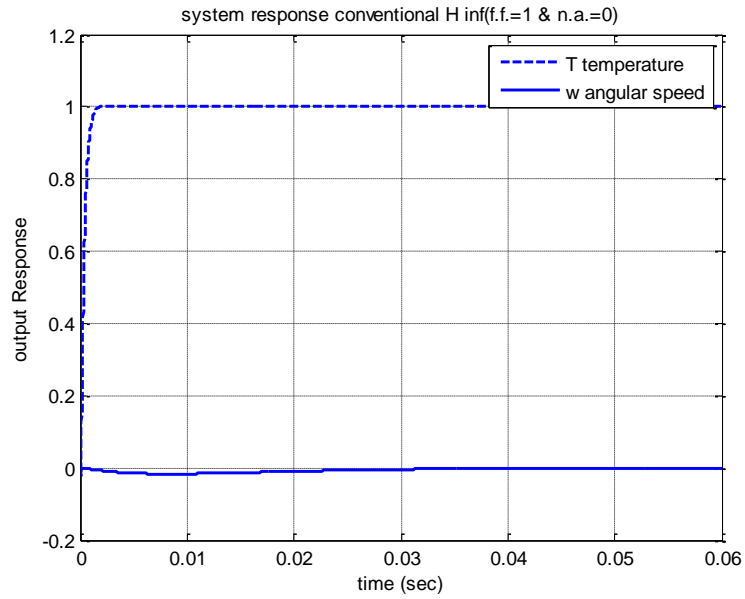


Figure 6.5: System response after applying a unit step change at $r_1(s)$

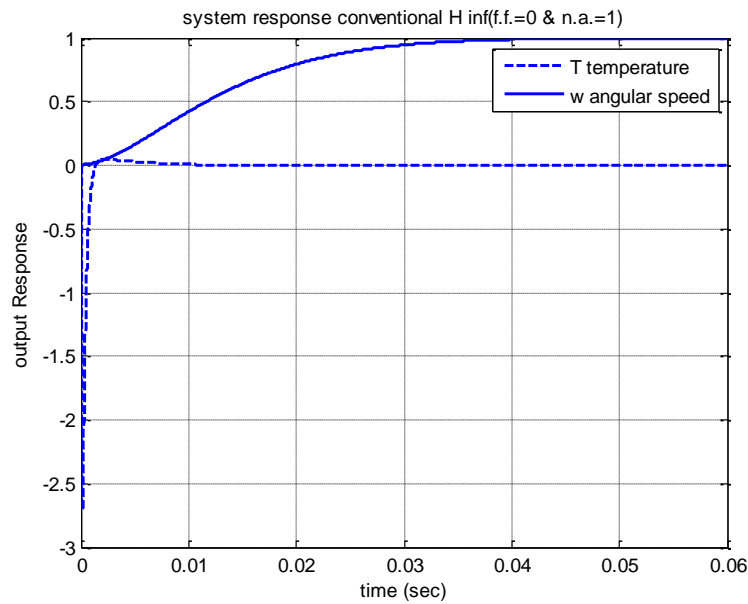


Figure 6.6: System response after applying a unit step change at $r_2(s)$

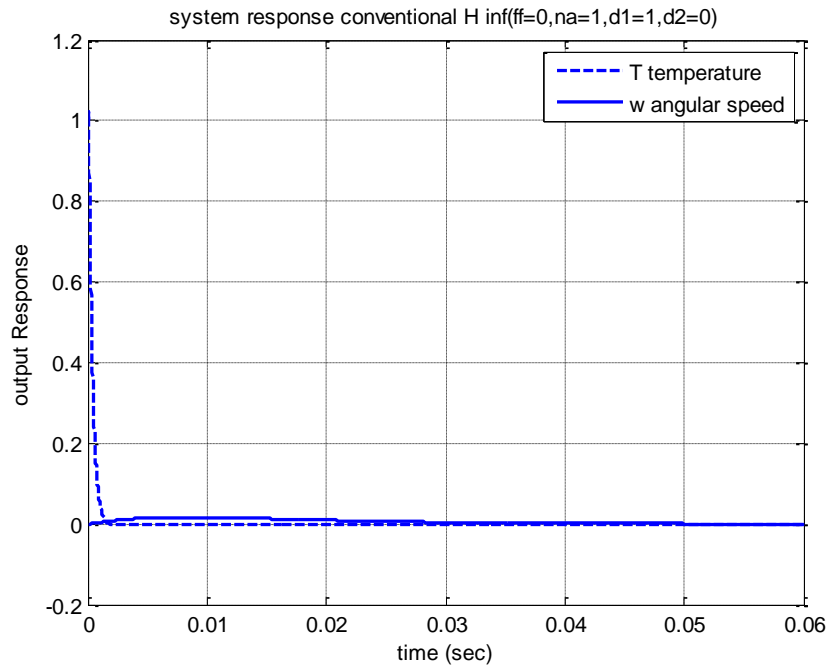


Figure 6.7: System response after applying a negative unit step at $\delta_1(s)$

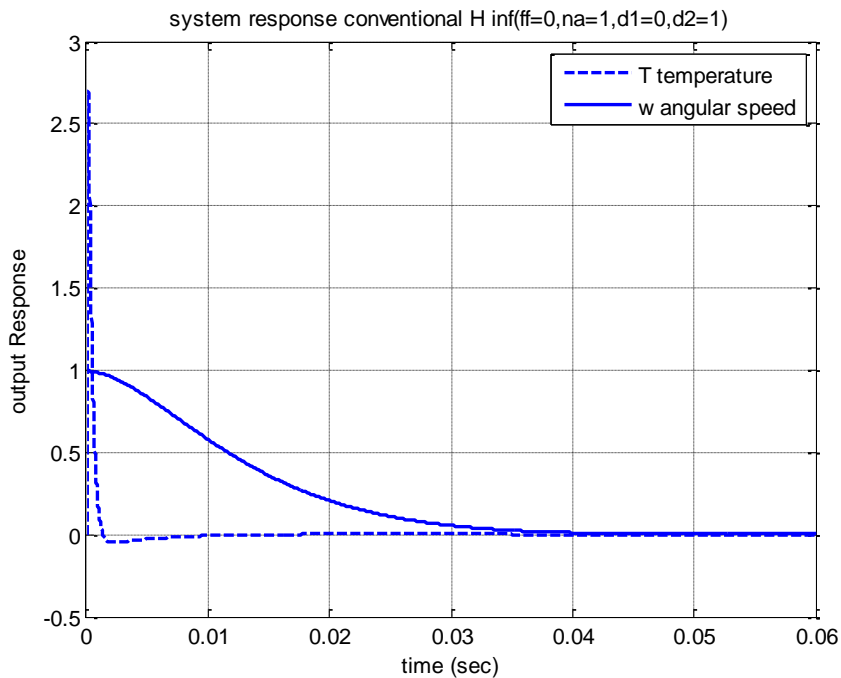


Figure 6.8: System response after applying a negative unit step at $\delta_2(s)$

A unit step input at $\delta_1(s)$ and $\delta_2(s)$ is used to show the system response following disturbances. Figures (6.7) and (6.8) show system's ability to suppress disturbances. Results show that the system with H infinity controller has a high steady state disturbance suppression behavior, but with initial transient reaction which exceed 100%. These disturbance transients would not be acceptable in practice.

Section seven:

Comparison Study

Controller implementation is a difficulty facing multivariable controller design methods but it is not the only one. Disturbance rejection and the controller consumption of energy are also difficulties in multivariable control system design. Concerning these factors the following comparison study between these methods, will be used in this research study.

7.1 Controller consumption of energy:

The control energy calculated after applying white noise at $\delta_1(s)$ and $\delta_2(s)$ is obtained by the following formula. According to the published paper of (R. Whalley and M. Ebrahimi ,2006)

$$E(t) = \int_{t=0}^{t=1} (u_1(t)^2 + u_2(t)^2) dt$$

Figure (7.1) shows a high level of control energy consumed in the H-infinity method with least control energy consumed by least effort method. The energy consumed by the controller will be converted to heat, noise and wear with increasing actuator activity. This affects the fuel consumption by gas turbine engine with reduced engine efficiency.

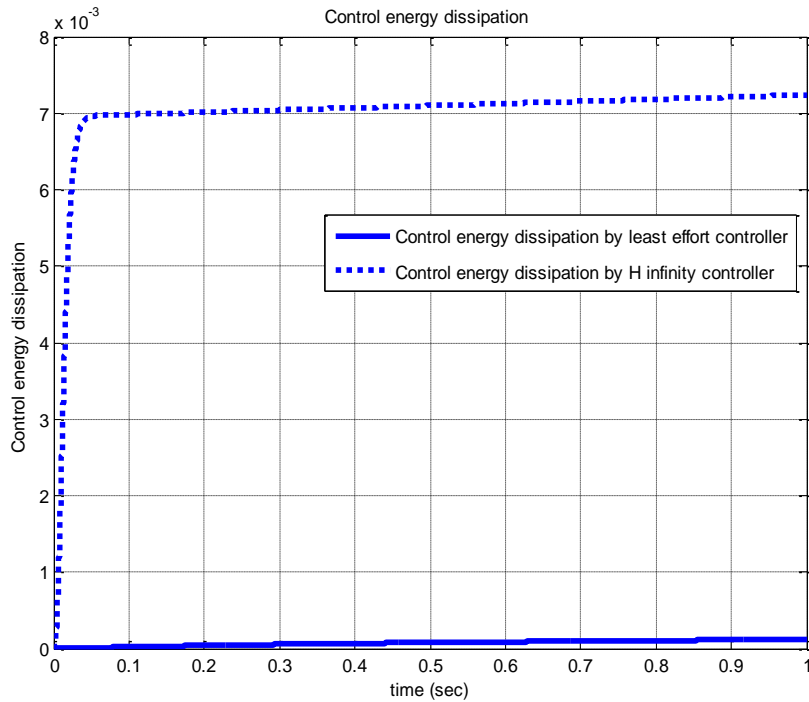


Figure 7.1: least effort and H infinity controllers' energy dissipation.

After examining the regulation methods, applicability is of vital importance; for instance. There is an extremely high order controller function, required for the H infinity method. Reduction methods can be claimed to provide lower order controller functions enabling simpler implementation. However, with this route stability of closed loop cannot even be guaranteed. Also, with reduction methods the selection of the weighting functions, the system response and the feedback algorithms are affected, as with all synthesis methods. When these properties are insufficient, an additional set of weights have to be selected until an adequate outcome is achieved. Essentially, this results is a reduction by trial and error means.

7.2 Controller implementation

The high order algorithms for the H infinity controller resulted in a fast system response, but produced difficulties in implementation with complicated controller functions giving difficulties in maintenance, drift, wear and aging. The simple algorithms obtained for the least effort technique does not involve these penalties.

The non-minimum phase characteristics shown in H-infinity controller algorithm gives additional difficulties, integrity and stability issues.

7.3 Disturbance rejection comparison

Figures 6.3 and 6.4 shows a pleasing result, for disturbance rejection with the least effort controller, giving a rejection performance of 91% and 92%, for the temperature and speed variations. This suppression of disturbances arising from the low gain compensators for the least effort technique.

Figures 6.7 and 6.8 shows disturbance rejection characteristics with a rejection performance of 100% in steady state for both figures. However, the initial reaction where there are huge impulse like, temperature response would not be acceptable as shown in figures 6.7 and 6.8.

Section eight

Conclusions and Recommendations

8.1 Conclusions:

In this study the employment of a gas turbine electric drive was investigated, for heavy duty vehicles.

This research investigates two control techniques. The first is the least effort method and then the H infinity method, for the gas turbine regulation. The system performance obtained using these regulators were distinctly different with varying controller algorithm complexity and control energy consumption. Therefore, the monotonically, diverging and significantly increasing amount of energy needed for the control purposes is significant.

Gas turbines achieve the highest power efficiency under full load conditions. The amount of power obtained from a low weight engine, with compactness and reliability has attracted considerable research attention.

The regulation of gas turbines depends on the closed loop strategy used and system robustness. This means avoiding high gain compensators and actuators in the control loops, with the use of accurate, efficient transducers and actuators.

The study is for heavy duty vehicles where relatively constant, smooth and rapid speed variations are required. The need for the closed loop system is to regulate the system response following reference changes and to minimize output interaction.

The results show how a least effort control techniques make the system faster with high stability response and good behavior. Also this results in a less interaction between the system outputs.

After this comparison, it can be concluded that since the performance shows a huge difference in response between the two methods, with the H infinity showing increased control energy consumption and actuator activity, generating noise and wear. Moreover, this additional energy consumption decreases the life cycle of the system while producing higher capital replacements and maintenance costs with lower system reliability. The previous conclusions are the results of poor design selection as well as decreases in the system life cycle duration.

8.2 Recommendations:

For multivariable systems, the least effort controller design method is recommended, especially for complicated applications. This method simplifies the controller structure, implementation, operating and maintenance procedures.

Gas turbine engines are recommended for long distance journeys way heavy duty automotives because of the engine efficiency under full load, constant speed conditions. Additionally, the engine output power and low weight are attractive properties.

For the least control energy dissipation and simplicity, the Least Effort design method, is usually used where simple control algorithms are needed while providing attractive characteristics of performance. This attribute and the actuator activity minimization, heat generation, wear, noise are all undesirable effects arising from the results of this study.

References:

Aström K. J. & Murray R. M., (2008), *Feedback Systems: An Introduction for Scientists and Engineers*, Princeton University Press, New Jersey, 2008

Astrom K. J. & Hagglund T., (1995), *PID Controllers*, 2nd Edition, Instrument Society of America, USA, 1995

Athans M., (1971), *Editorial on the LQG problem*, IEEE Transection. Automation Control. volume 16, no. 6

Bansal A. and Sharma V.,(2013), *Design and Analysis of Robust H-infinity Controller*, National Conference on Emerging Trends in Electrical, Instrumentation & Communication Engineering, Vol.3, No.2, 2013

Bryson, A. E. (1996). *Optimal Control -1950 to 1985*. IEEE Control Systems (Volume: 16, Issue: 3, Jun 1996)

Chiras, N. (2002), *Linear and nonlinear modeling of gas turbines*. Ph.D. Thesis. University of Glamorgan, 2002. "[online] (accessed 25 March 2016)

David John Bell, (1988). *Design of Modern Control Systems*, Peter Peregrinus Ltd.,London, United Kingdom

Dingyu X, YangQuan C and Derek P, (2007), *Linear Feedback Control Analysis and Design with MATLAB*, Siam, Philadelphia, 2007.

Dorf, R.C. and Bishop, R.H. (2008), *Modern Control Systems*. Pearson Education Inc. New York.

El-Hassan, T. (2012). *A Design Study for Multivariable Feedback Control System Regulation for Aircraft Turbo-Jet Engines*. MSc. Dissertation, The British University in Dubai, Dubai.

Edmunds, J.M. and Munro, N., (2009) *Control Systems, Robotics and Automation- Design Techniques in the Frequency Domain*, Vlo. 8, Control

System Center, UMIST, UK, Encyclopedia of Life Support Systems (EOLSS) chapter.

Foss A. S., Edmunds J. M. & Kouvaritakis B,(1980). *Multivariable Control System for Two-Bed Reactors by the Characteristic Locus Method*. Ind. Eng. Chem. Fundamen.,

Gershon E; Shaked U. & Yaesh I. (2005), *H-infinity Control and Estimation of State-multiplicative Linear Systems*, Springer-Verlag London Limited, London

Gilbert G. E., (1962), *Controllability and observability in multivariable control systems*, Journal of the Society for Industrial and Applied Mathematics Series A Control, 1(2), 128–151. (24 pages), Submitted: 05 July 1962, Published online: 18 July 2006

Gopal M.,(2008), *Control Systems: Principles and Design*, Tata McGraw-Hill Publishing Company Limited, New Delhi,

Leigh J. R., (1987), *Applied Control Theory* - 2nd edition, Peter Peregrinus Ltd.,London, United Kingdom

Jaw L.C. and Garg S., (2005), *Proportional Control Technology Development in the United States: A Historical Perspective*. NASA/TM-2005-213978

Johnson M. A. & Moradi M. H.,(2005), *PID Control New Identification and Design Methods*, Springer-Verlag London Limited, London ,2005

John e. Bibel & D. Stephen Malyevac, (1992), *Guidelines For The Selection Of Weighting Functions For H-Infinity Control*, Naval Surface Warfare Center Dahlgren Division, Dahlgren. Virginia

O'Reilly J., (1987), *Multivariable Control for Industrial Applications*, Peter Peregrinus Ltd.,London, United Kingdom

Kalman R. E., (1960), *A new approach to linear filtering and prediction problems*. Transactions of the ASME, Journal of Basic Engineering, March 1960 issue

Hangos K. M.; Lakner R. & Gerzson M. (2001). *Intelligent Control Systems: An Introduction with Examples*. Kluwer Academic Publishers, Dordrecht

Hangos K. M.; Bokor J. & Szederkényi G. (2004). *Analysis and Control of Nonlinear Process Systems*. Springer-Verlag London Limited.

Lehto, S.,(2012), *Chrysler's Turbine Car: The Rise and Fall of Detroit's Coolest Creation*, Chicago Review Press, 2012.

Meherwan P. Boyce., (2006), *Gas Turbine Engineering Handbook*, Gulf Professional Publishing, Texas.

Megdadi E., Whalley R. & Ebrahimi K. M.,(2016), *Multivariable Regulation of Gas Turbines for Automotive Applications*, Paper submitted to PMC2016, 3rd Biennial International Powertrain Modeling and Control Conference, Loughborough, UK, 2016.

Nof, Shimon Y. (Ed.), (2009), *Springer Handbook of Automation*, Springer, London

Norman S. Nise, (2006), *Control Systems Engineering*, 6th edition, John Wiley & Sons, Inc,USA, 2006

Nye. D, (2008), *BRM- The Saga of British Racing Motors*, Vol. 2, Motor Racing Publications, 2008.

Nyquist, H. (January 1932). *Regeneration Theory*. The Bell System Technical Journal (Volume: 11, Issue: 1, Jan. 1932) Publisher: Alcatel-Lucent, USA: Retrieved December 5, 2012. on Alcatel-Lucent website.

Otto Mayr., (1971), *Adam Smith and the Concept of the Feedback System: Economic Thought and Technology in 18th-Century Britain*. Technology and Culture journal, vol. 12, no. 1, 1971, pp. 1–22. www.jstor.org/stable/3102276.

Patel R V & Munro N, (1982). *Multivariable System Theory and Design*, Academic Press, London, 1982.

Phillips P. A., (2006), *Design, Development and Application of Vehicle Gas Turbine Engines*, Proceedings of the Institution of Mechanical Engineers: Automobile Division, Vol 181, Issue 1, pp. 149 – 172, February-03-2006

Robert L. Williams & Douglas A. Lawrence, (2007), *Linear State-Space Control Systems*, John Wiley & Sons, Inc., New Jersey

Routh, E. J. (1877). *A Treatise on the Stability of a Given State of Motion: Particularly Steady Motion*. Macmillan and co. London

Ross, I. M. (2009). *A Primer on Pontryagin's Principle in Optimal Control*. Collegiate Publishers. ISBN 978-0-9843571-0-9.

Stefano Longo; Tingli Su; Guido Herrmann & Phil Barber, (2013), *Optimal and Robust Scheduling for Networked Control Systems*, CRC Press Taylor & Francis Group, LLC. NW USA.

Skogestad S. & Postlethwaite I, (1996), *Multivariable Feedback Control: Analysis and Design*, J Wiley and Son, London, 1996.

Saravanamuttoo H.I.H. Rogers G.F.C., Cohen, H., Straznicky, P., (2008), *Gas Turbine Theory*, Prentice Hall; Edition 6, 2008.

U.S. Department of Transportation Federal Aviation Administration Flight Standards Service, (2004), *Airplane Flying Handbook*, Airman Testing Standards Branch, Oklahoma City, 2004.

Westphal L. C., (2001), *Handbook of Control Systems Engineering*, Kluwer Academic Publishers, USA

Whalley, R.(1978).*Spectral Factorization of the Transfer Matrix*. Proc. IMechE ,vol.192,

Whalley, R., (2016), *Multivariable systems and control*, ENGG506 Lecture notes distributed in the module, the British University in Dubai, Dubai, October 2015.

Whalley, R., (2016), *State Space and Multivariable systems*, ENGG505 Lecture notes distributed in the module, the British University in Dubai, Dubai, September 2015.

Whalley, R and Ebrahimi, M, (2006), *Multivariable System Regulation*, Proc. IMechE, Part C, Journal of Mechanical Engineering Science, Vol. 220, No.5, 2006, pp. 653-667.

Whalley R. & Ebrahimi M., (2004), *Automotive Gas Turbine Regulation*, IEEE Trans. Contr. Syst. Technol., (2004), pp. 465-473.

Whalley R.; Ebrahimi M., (2000), *Process System Regulation with Minimum Control Effort*, Proceedings of the IMechE Part E Journal of Process Mechanical Engineering, Volume 214, 2000, pp. 245-256.

Whalley, R., (2012), *Integrity Analysis for Multivariable Feedback Systems*, The 8th WSEAS International Conference on dynamical systems and control, Portugal,

Whalley, R.; Abdul-Ameer, A.; Ebrahimi, M. & Nikranjbar, A. (2010). *Winder Control using a Ward-Leondard System*. Int.Journal Industrial Systems Engineering , vol.6, No.2

Whalley, R and El-Hassan, T, (2012), *Turbo-Jet Engine Multivariable Control*, Proc. WCECS, Conference of World Congress on Engineering and Computer Science, Vol. II, 2012.

Wheaton. J, " *Rover Turbine Cars* ", (<http://www.rover.org.nz/pages/jet/jet5.htm>), accessed 25 March 2016.

Appendix

1. MatLab code

MATLAB shortcut of matrix laboratory is a programming language produced by MathWorks Inc.. it is invented for numerical computing with optional toolboxes. Nowadays, millions using this programming language in academic and industrial sectors.

The following code is the least effort controller code used for simulation in this research.

1.1 least effort controller:

```
2. s = tf('s');
3. G = [0.967*10^6/(s+40) -
      8.1248*(s+3.27)/(s+0.95);8.82*10^6*(s+31.42)/((s+1.55)*(s+40)*(s+187
      .4)) 50.2/(s+1.55)];
4. G0=[24175 -27.96641684;2.385137879987606e+04 32.387];
5. bs = tf([1 1.55],[1 588.95 75870.5 11618]); %Expanded form
      %d(s)=(s+1.55)(s+400)(s+187.4)
6. b0=1.09*10^4 % from the graph of rlocus(bs) the rang (0 to
      2.8*10^6 to ) for b
7. b=b0*[1;1.55]
8. Q=[(0.918*10^6-26.5638*n) (2772*10^5+9424.5*n);(0.967*10^6-8.125*n)
      (88.2*10^5+50.20*n)];
9.
10. step(G)
11. figure
12. rlocus(bs)
13. figure
14. J(n)=(1+n^2)*transpose(b)*transpose(inv(Q))*inv(Q)*b;
15. JR = vpa(J)
16. dJ=diff(J,n);
17. ezplot(J); %% ezplot(f,[xmin,xmax,ymin,ymax])
18. ylabel('performance index J')
19. grid on
```

```

20.
21. [symNum,symDen] = numden(J(n)); %Get num and den of Symbolic TF
22. TFnum = sym2poly(symNum); %Convert Symbolic num to
    polynomial
23. TFden = sym2poly(symDen); %Convert Symbolic den to
    polynomial
24. Js =tf(TFnum,TFden)
25. solx = solve(dJ==0, n)
26. Jvalu=[J(solx(1,1)) J(solx(2,1)) J(solx(3,1)) J(solx(4,1))]
27. nv=-0.00000747416067 %or per solx = solve(dJ==0, n)
28. Qv=subs(Q,nv);
29. Qv1=double(Qv)
30. invQv1=double(inv(Qv))
31. h=inv(Qv)*b
32. hi=double(inv(Qv))*b
33. hh=double(h)
34. hs=[hi(1,1)*(s+0.95)/((s+1.55)*(s+187.4)) hi(2,1)]
35. h0=[hh(1,1)/0.95;hh(2,1)/(1.55*187.4)]
36.
37. k1=1;
38. k2=nv;
39. k=[k1;k2]
40. ki=double(k)
41. ks=[ki(1,1)*(s+40)/(s+400);ki(2,1)/(s+400)]
42. k0=[k1/10;k2/400]
43.
44. F = [0.9 0;0 0.9];
45. Ss=[1 0.1;0.1 1];
46. I=[1 0;0 1];
47.
48. P=(inv(G0)+k0 * h0')*Ss*inv(I-F*Ss);
49. H=inv(P)*(k * h')+F
50.
51. PM = double(P)

```

```

52. HM = double(H)
53.
54. Hs=inv(PM)*(ks*hs)+F
55. [numh11,denh11] = tfdata(Hs(1,1))
56. [numh21,denh21] = tfdata(Hs(2,1))
57. [numh12,denh12] = tfdata(Hs(1,2))
58. [numh22,denh22] = tfdata(Hs(2,2))
59.
60. set_param('desertation2full2ss/P11','Gain','PM(1,1)')
61. set_param('desertation2full2ss/P12','Gain','PM(1,2)')
62. set_param('desertation2full2ss/P21','Gain','PM(2,1)')
63. set_param('desertation2full2ss/P22','Gain','PM(2,2)')
64.
65. set_param('desertation2full2ss/TF11','Numerator','numh11{1}','Denominator','denh11{1}'); % TF=H(s)
66. set_param('desertation2full2ss/TF21','Numerator','numh21{1}','Denominator','denh21{1}'); % TF=H(s)
67. set_param('desertation2full2ss/TF12','Numerator','numh12{1}','Denominator','denh12{1}'); % TF=H(s)
68. set_param('desertation2full2ss/TF22','Numerator','numh22{1}','Denominator','denh22{1}'); % TF=H(s)
69.
70. set_param('desertation2full2ss/ffStep1','after','1')
71. set_param('desertation2full2ss/naStep2','after','0')
72.
73. set_param('desertation2full2ss/d1','after','0')
74. set_param('desertation2full2ss/d2','after','0')
75.
76. sim('desertation2full2ss')
77.
78. figure
79. p=plot(tout,T1simout,'b--',tout,w2simout,'b-','LineWidth',2)
80. legend('T temperature f=.9','w angular speed f=.9')
81. xlabel('time (sec)')

```

```

82. ylabel('output Response')
83. title('system response conventional(K(s),H(s)) (f.f.=1 & n.a.=0)')
84. grid on
85. hold
86.
87. F = [0.8 0;0 0.8];
88. P=(inv(G0)+k0 * h0')*Ss*inv(I-F*Ss);
89. Hs=inv(PM)*(ks*hs)+F;
90.
91. PM = double(P)
92. set_param('desertation2full2ss/P11','Gain','PM(1,1)')
93. set_param('desertation2full2ss/P12','Gain','PM(1,2)')
94. set_param('desertation2full2ss/P21','Gain','PM(2,1)')
95. set_param('desertation2full2ss/P22','Gain','PM(2,2)')
96.
97. [numh11,denh11] = tfdata(Hs(1,1))
98. [numh21,denh21] = tfdata(Hs(2,1))
99. [numh12,denh12] = tfdata(Hs(1,2))
100. [numh22,denh22] = tfdata(Hs(2,2))
101. set_param('desertation2full2ss/TF11','Numerator','numh11{1}','Den
    ominator','denh11{1}'); % TF=H(s)
102. set_param('desertation2full2ss/TF21','Numerator','numh21{1}','Den
    ominator','denh21{1}');
103. set_param('desertation2full2ss/TF12','Numerator','numh12{1}','Den
    ominator','denh12{1}');
104. set_param('desertation2full2ss/TF22','Numerator','numh22{1}','Den
    ominator','denh22{1}');
105.
106. sim( 'desertation2full2ss' )
107.
108. p=plot(tout,T1simout,'r--',tout,w2simout,'r-','LineWidth',2)
109. legend('T temperature f=.8','w angular speed f=.8')
110.
111. F = [0.5 0;0 0.5];

```

```

112. P=(inv(G0)+k0 * h0')*Ss*inv(I-F*Ss);
113. Hs=inv(PM)*(ks*hs)+F;
114.
115. PM = double(P)
116. set_param('desertation2full2ss/P11','Gain','PM(1,1)')
117. set_param('desertation2full2ss/P12','Gain','PM(1,2)')
118. set_param('desertation2full2ss/P21','Gain','PM(2,1)')
119. set_param('desertation2full2ss/P22','Gain','PM(2,2)')
120.
121. [numh11,denh11] = tfdata(Hs(1,1))
122. [numh21,denh21] = tfdata(Hs(2,1))
123. [numh12,denh12] = tfdata(Hs(1,2))
124. [numh22,denh22] = tfdata(Hs(2,2))
125. set_param('desertation2full2ss/TF11','Numerator','numh11{1}','Den
    ominator','denh11{1}'); % TF=H(s)
126. set_param('desertation2full2ss/TF21','Numerator','numh21{1}','Den
    ominator','denh21{1}');
127. set_param('desertation2full2ss/TF12','Numerator','numh12{1}','Den
    ominator','denh12{1}');
128. set_param('desertation2full2ss/TF22','Numerator','numh22{1}','Den
    ominator','denh22{1}');
129.
130. sim( 'desertation2full2ss' )
131.
132. p=plot(tout,T1simout,'g--',tout,w2simout,'g-','LineWidth',2)
133. legend('T temperature f=.5','w angular speed f=.5')
134.
135. legend('T temperature f=0.9','w angular speedf=0.9','T
    temperature f=0.8','w angular speedf=0.8','T temperature f=0.5','w
    angular speedf=0.5')
136.
137. %%%%%%%%% ff=0 na=1
138.
139. set_param('desertation2full2ss/ffStep1','after','0')

```

```

140. set_param('desertation2full2ss/naStep2','after','1')
141.
142. set_param('desertation2full2ss/d1','after','0')
143. set_param('desertation2full2ss/d2','after','0')
144.
145. F = [0.9 0;0 0.9];
146. P=(inv(G0)+k0 * h0')*Ss*inv(I-F*Ss);
147. Hs=inv(PM)*(ks*hs)+F;
148.
149. PM = double(P)
150. set_param('desertation2full2ss/P11','Gain','PM(1,1)')
151. set_param('desertation2full2ss/P12','Gain','PM(1,2)')
152. set_param('desertation2full2ss/P21','Gain','PM(2,1)')
153. set_param('desertation2full2ss/P22','Gain','PM(2,2)')
154.
155. [numh11,denh11] = tfdata(Hs(1,1))
156. [numh21,denh21] = tfdata(Hs(2,1))
157. [numh12,denh12] = tfdata(Hs(1,2))
158. [numh22,denh22] = tfdata(Hs(2,2))
159. set_param('desertation2full2ss/TF11','Numerator','numh11{1}','Den
    ominator','denh11{1}'); % TF=H(s)
160. set_param('desertation2full2ss/TF21','Numerator','numh21{1}','Den
    ominator','denh21{1}');
161. set_param('desertation2full2ss/TF12','Numerator','numh12{1}','Den
    ominator','denh12{1}');
162. set_param('desertation2full2ss/TF22','Numerator','numh22{1}','Den
    ominator','denh22{1}');
163.
164. sim( 'desertation2full2ss' )
165.
166. figure
167. p=plot(tout,T1simout,'b--',tout,w2simout,'b-','LineWidth',2)
168.
169. legend('T temperature f=.9','w angular speed f=.9')

```

```

170. xlabel('time (sec)')
171. ylabel('output Response')
172. title('system response conventional(K(s),H(s) (f.f.=0 & n.a.=1)')
173. grid on
174.
175. hold
176.
177. F = [0.8 0;0 0.8];
178. P=(inv(G0)+k0 * h0')*Ss*inv(I-F*Ss);
179. Hs=inv(PM)*(ks*hs)+F;
180.
181. PM = double(P)
182. set_param('desertation2full2ss/P11','Gain','PM(1,1)')
183. set_param('desertation2full2ss/P12','Gain','PM(1,2)')
184. set_param('desertation2full2ss/P21','Gain','PM(2,1)')
185. set_param('desertation2full2ss/P22','Gain','PM(2,2)')
186.
187. [numh11,denh11] = tfdata(Hs(1,1))
188. [numh21,denh21] = tfdata(Hs(2,1))
189. [numh12,denh12] = tfdata(Hs(1,2))
190. [numh22,denh22] = tfdata(Hs(2,2))
191. set_param('desertation2full2ss/TF11','Numerator','numh11{1}','Den
    ominator','denh11{1}'); % TF=H(s)
192. set_param('desertation2full2ss/TF21','Numerator','numh21{1}','Den
    ominator','denh21{1}');
193. set_param('desertation2full2ss/TF12','Numerator','numh12{1}','Den
    ominator','denh12{1}');
194. set_param('desertation2full2ss/TF22','Numerator','numh22{1}','Den
    ominator','denh22{1}');
195.
196. sim( 'desertation2full2ss' )
197.
198. p88=plot(tout,T1simout,'r--',tout,w2simout,'r-','LineWidth',2)
199. legend('T temperature f=.8','w angular speed f=.8')

```

```

200.
201. F = [0.5 0;0 0.5];
202. P=(inv(G0)+k0 * h0')*Ss*inv(I-F*Ss);
203. Hs=inv(PM)*(ks*hs)+F;
204.
205. PM = double(P)
206. set_param('desertation2full2ss/P11','Gain','PM(1,1)')
207. set_param('desertation2full2ss/P12','Gain','PM(1,2)')
208. set_param('desertation2full2ss/P21','Gain','PM(2,1)')
209. set_param('desertation2full2ss/P22','Gain','PM(2,2)')
210.
211. [numh11,denh11] = tfdata(Hs(1,1))
212. [numh21,denh21] = tfdata(Hs(2,1))
213. [numh12,denh12] = tfdata(Hs(1,2))
214. [numh22,denh22] = tfdata(Hs(2,2))
215. set_param('desertation2full2ss/TF11','Numerator','numh11{1}','Den
    ominator','denh11{1}'); % TF=H(s)
216. set_param('desertation2full2ss/TF21','Numerator','numh21{1}','Den
    ominator','denh21{1}');
217. set_param('desertation2full2ss/TF12','Numerator','numh12{1}','Den
    ominator','denh12{1}');
218. set_param('desertation2full2ss/TF22','Numerator','numh22{1}','Den
    ominator','denh22{1}');
219.
220. sim( 'desertation2full2ss' )
221.
222. p=plot(tout,T1simout,'g--',tout,w2simout,'g-','LineWidth',2)
223. legend('T temperature f=.5','w angular speed f=.5')
224.
225. legend('T temperature f=0.9','w angular speedf=0.9','T
    temperature f=0.8','w angular speedf=0.8','T temperature f=0.5','w
    angular speedf=0.5')
226.
227. %%%% dis ff=0,na=0,d1=-1,d2=0

```



```

228.
229. set_param('desertation2full2ss/ffStep1','after','0')
230. set_param('desertation2full2ss/naStep2','after','0')
231.
232. set_param('desertation2full2ss/d1','after','-1')
233. set_param('desertation2full2ss/d2','after','0')
234.
235. F = [0.9 0;0 0.9];
236. P=(inv(G0)+k0 * h0')*Ss*inv(I-F*Ss);
237. Hs=inv(PM)*(ks*hs)+F;
238.
239. PM = double(P)
240. set_param('desertation2full2ss/P11','Gain','PM(1,1)')
241. set_param('desertation2full2ss/P12','Gain','PM(1,2)')
242. set_param('desertation2full2ss/P21','Gain','PM(2,1)')
243. set_param('desertation2full2ss/P22','Gain','PM(2,2)')
244.
245. [numh11,denh11] = tfdata(Hs(1,1))
246. [numh21,denh21] = tfdata(Hs(2,1))
247. [numh12,denh12] = tfdata(Hs(1,2))
248. [numh22,denh22] = tfdata(Hs(2,2))
249. set_param('desertation2full2ss/TF11','Numerator','numh11{1}','Den
    ominator','denh11{1}'); % TF=H(s)
250. set_param('desertation2full2ss/TF21','Numerator','numh21{1}','Den
    ominator','denh21{1}');
251. set_param('desertation2full2ss/TF12','Numerator','numh12{1}','Den
    ominator','denh12{1}');
252. set_param('desertation2full2ss/TF22','Numerator','numh22{1}','Den
    ominator','denh22{1}');
253.
254. sim( 'desertation2full2ss' )
255.
256. figure
257. p=plot(tout,T1simout,'b--',tout,w2simout,'b-','LineWidth',2)

```

```

258.
259. legend('T temperature f=.9','w angular speed f=.9')
260. xlabel('time (sec)')
261. ylabel('output Response')
262. title('sys.res.conven. (K(s),H(s) (ff=0,na=0,d1=-1,d2=0)')
263. grid on
264.
265. hold
266.
267. F = [0.8 0;0 0.8];
268. P=(inv(G0)+k0 * h0')*Ss*inv(I-F*Ss);
269. Hs=inv(PM)*(ks*hs)+F;
270.
271. PM = double(P)
272. set_param('desertation2full2ss/P11','Gain','PM(1,1)')
273. set_param('desertation2full2ss/P12','Gain','PM(1,2)')
274. set_param('desertation2full2ss/P21','Gain','PM(2,1)')
275. set_param('desertation2full2ss/P22','Gain','PM(2,2)')
276.
277. [numh11,denh11] = tfdata(Hs(1,1))
278. [numh21,denh21] = tfdata(Hs(2,1))
279. [numh12,denh12] = tfdata(Hs(1,2))
280. [numh22,denh22] = tfdata(Hs(2,2))
281. set_param('desertation2full2ss/TF11','Numerator','numh11{1}','Den
    ominator','denh11{1}'); % TF=H(s)
282. set_param('desertation2full2ss/TF21','Numerator','numh21{1}','Den
    ominator','denh21{1}');
283. set_param('desertation2full2ss/TF12','Numerator','numh12{1}','Den
    ominator','denh12{1}');
284. set_param('desertation2full2ss/TF22','Numerator','numh22{1}','Den
    ominator','denh22{1}');
285.
286. sim( 'desertation2full2ss' )
287.

```

```

288. p88=plot(tout,T1simout,'r--',tout,w2simout,'r-','LineWidth',2)
289.
290. legend('T temperature f=.8','w angular speed f=.8')
291.
292. F = [0.5 0;0 0.5];
293. P=(inv(G0)+k0 * h0')*Ss*inv(I-F*Ss);
294. Hs=inv(PM)*(ks*hs)+F;
295.
296. PM = double(P)
297. set_param('desertation2full2ss/P11','Gain','PM(1,1)')
298. set_param('desertation2full2ss/P12','Gain','PM(1,2)')
299. set_param('desertation2full2ss/P21','Gain','PM(2,1)')
300. set_param('desertation2full2ss/P22','Gain','PM(2,2)')
301.
302. [numh11,denh11] = tfdata(Hs(1,1))
303. [numh21,denh21] = tfdata(Hs(2,1))
304. [numh12,denh12] = tfdata(Hs(1,2))
305. [numh22,denh22] = tfdata(Hs(2,2))
306. set_param('desertation2full2ss/TF11','Numerator','numh11{1}','Den
    ominator','denh11{1}'); % TF=H(s)
307. set_param('desertation2full2ss/TF21','Numerator','numh21{1}','Den
    ominator','denh21{1}');
308. set_param('desertation2full2ss/TF12','Numerator','numh12{1}','Den
    ominator','denh12{1}');
309. set_param('desertation2full2ss/TF22','Numerator','numh22{1}','Den
    ominator','denh22{1}');
310.
311. sim( 'desertation2full2ss' )
312.
313. p=plot(tout,T1simout,'g--',tout,w2simout,'g-','LineWidth',2)
314.
315. legend('T temperature f=.5','w angular speed f=.5')
316.

```

```

317. legend('T temperature f=0.9','w angular speedf=0.9','T
      temperature f=0.8','w angular speedf=0.8','T temperature f=0.5','w
      angular speedf=0.5')
318.
319. %%%% dis ff=0,na=0,d1=0,d2=-1
320.
321. set_param('desertation2full2ss/ffStep1','after','0')
322. set_param('desertation2full2ss/naStep2','after','0')
323.
324. set_param('desertation2full2ss/d1','after','0')
325. set_param('desertation2full2ss/d2','after','-1')
326.
327. F = [0.9 0;0 0.9];
328. P=(inv(G0)+k0 * h0')*Ss*inv(I-F*Ss);
329. Hs=inv(PM)*(ks*hs)+F;
330.
331. PM = double(P)
332. set_param('desertation2full2ss/P11','Gain','PM(1,1)')
333. set_param('desertation2full2ss/P12','Gain','PM(1,2)')
334. set_param('desertation2full2ss/P21','Gain','PM(2,1)')
335. set_param('desertation2full2ss/P22','Gain','PM(2,2)')
336.
337. [numh11,denh11] = tfdata(Hs(1,1))
338. [numh21,denh21] = tfdata(Hs(2,1))
339. [numh12,denh12] =tfdata(Hs(1,2))
340. [numh22,denh22] = tfdata(Hs(2,2))
341. set_param('desertation2full2ss/TF11','Numerator','numh11{1}','Den
      ominator','denh11{1}'); % TF=H(s)
342. set_param('desertation2full2ss/TF21','Numerator','numh21{1}','Den
      ominator','denh21{1}');
343. set_param('desertation2full2ss/TF12','Numerator','numh12{1}','Den
      ominator','denh12{1}');
344. set_param('desertation2full2ss/TF22','Numerator','numh22{1}','Den
      ominator','denh22{1}');

```

```

345.
346. sim( 'desertation2full2ss' )
347.
348. figure
349. p=plot(tout,T1simout,'b--',tout,w2simout,'b-','LineWidth',2)
350. legend('T temperature f=.9','w angular speed f=.9')
351. xlabel('time (sec)')
352. ylabel('output Response')
353. title('sys.res.conven.(K(s),H(s) (ff=0,na=0,d1=0,d2=-1)')
354. grid on
355.
356. hold
357.
358. F = [0.8 0;0 0.8];
359. P=(inv(G0)+k0 * h0')*Ss*inv(I-F*Ss);
360. Hs=inv(PM)*(ks*hs)+F;
361.
362. PM = double(P)
363. set_param('desertation2full2ss/P11','Gain','PM(1,1)')
364. set_param('desertation2full2ss/P12','Gain','PM(1,2)')
365. set_param('desertation2full2ss/P21','Gain','PM(2,1)')
366. set_param('desertation2full2ss/P22','Gain','PM(2,2)')
367.
368. [numh11,denh11] = tfdata(Hs(1,1))
369. [numh21,denh21] =tfdata(Hs(2,1))
370. [numh12,denh12] = tfdata(Hs(1,2))
371. [numh22,denh22] = tfdata(Hs(2,2))
372. set_param('desertation2full2ss/TF11','Numerator','numh11{1}','Den
    ominator','denh11{1}'); % TF=H(s)
373. set_param('desertation2full2ss/TF21','Numerator','numh21{1}','Den
    ominator','denh21{1}');
374. set_param('desertation2full2ss/TF12','Numerator','numh12{1}','Den
    ominator','denh12{1}');

```

```

375. set_param('desertation2full2ss/TF22','Numerator','numh22{1}','Den
    ominator','denh22{1}');
376.
377. sim( 'desertation2full2ss' )
378.
379. p88=plot(tout,T1simout,'r--',tout,w2simout,'r-','LineWidth',2)
380. legend('T temperature f=.8','w angular speed f=.8')
381.
382.
383. F = [0.5 0;0 0.5];
384. P=(inv(G0)+k0 * h0')*Ss*inv(I-F*Ss);
385. Hs=inv(PM)*(ks*hs)+F;
386.
387. PM = double(P)
388. set_param('desertation2full2ss/P11','Gain','PM(1,1)')
389. set_param('desertation2full2ss/P12','Gain','PM(1,2)')
390. set_param('desertation2full2ss/P21','Gain','PM(2,1)')
391. set_param('desertation2full2ss/P22','Gain','PM(2,2)')
392.
393. [numh11,denh11] = tfdata(Hs(1,1))
394. [numh21,denh21] = tfdata(Hs(2,1))
395. [numh12,denh12] = tfdata(Hs(1,2))
396. [numh22,denh22] = tfdata(Hs(2,2))
397. set_param('desertation2full2ss/TF11','Numerator','numh11{1}','Den
    ominator','denh11{1}'); % TF=H(s)
398. set_param('desertation2full2ss/TF21','Numerator','numh21{1}','Den
    ominator','denh21{1}');
399. set_param('desertation2full2ss/TF12','Numerator','numh12{1}','Den
    ominator','denh12{1}');
400. set_param('desertation2full2ss/TF22','Numerator','numh22{1}','Den
    ominator','denh22{1}');
401.
402. sim( 'desertation2full2ss' )
403.

```

```

404. p=plot(tout,T1simout,'g--',tout,w2simout,'g-','LineWidth',2)
405. legend('T temperature f=.5','w angular speed f=.5')
406.
407. legend('T temperature f=0.9','w angular speedf=0.9','T
temperature f=0.8','w angular speedf=0.8','T temperature f=0.5','w
angular speedf=0.5')

```

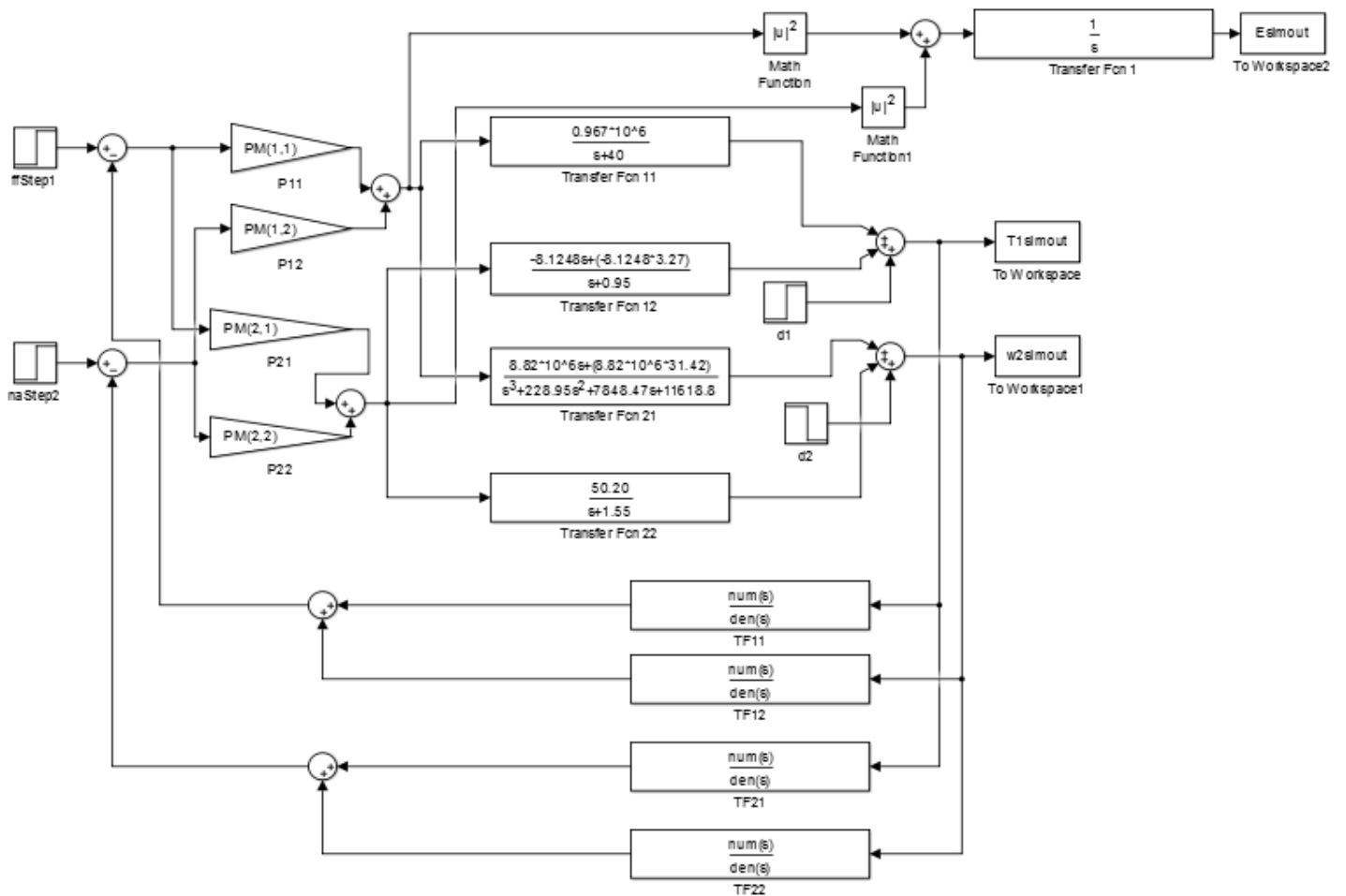


Figure A.1: least effort controller simulation model

1.2H infinity controller code:

```
2 format short e;
3 syms s;
4 s = tf('s');
5 G = [0.967*10^6/(s+40) -
      8.1248*(s+3.27)/(s+0.95); 8.82*10^6*(s+31.42)/((s+1.55)*(s+40)*(s+187.4))
      50.2/(s+1.55)];
6 G0=[24175 -27.96641684; 2.385137879987606e+04 32.387];
7
8 g11=tf(0.967*10^6/(s+40))
9 g12=tf(-8.1248*(s+3.27)/(s+0.95))
10 g21=tf(8.82*10^6*(s+31.42)/((s+1.55)*(s+40)*(s+187.4)))
11 g22=tf(50.2/(s+1.55))
12 Gh=[g11 g12; g21 g22];
13
14 W1=[100/(s+0.5), 0; 0, 100/(s+1)];
15 W2=[tf(1e-5), 0; 0, tf(1e-5)]; W3=[s/1000, 0; 0, s/200];
16 Tss=augtf(Gh,W1,W2,W3); [g,Gc]=hinftopt(Tss); zpk(Gc(1,2))
17
18 step(feedback(Gh*Gc,eye(2)),0.1)
19 figure
20
21 step(G)
22 figure
23
24 Hs=Gc
25 [numh11,denh11] = tfdata(Hs(1,1))
26 [numh21,denh21] = tfdata(Hs(2,1))
27 [numh12,denh12] = tfdata(Hs(1,2))
28 [numh22,denh22] = tfdata(Hs(2,2))
29
30 set_param('desertation2full2ss2/TF11','Numerator','numh11{1}','Denominator',
    'denh11{1}'); % TF=H(s)
```



```

31 set_param('desertation2full2ss2/TF21','Numerator','numh21{1}','Denominator
    ','denh21{1}');
32 set_param('desertation2full2ss2/TF12','Numerator','numh12{1}','Denominator
    ','denh12{1}');
33 set_param('desertation2full2ss2/TF22','Numerator','numh22{1}','Denominator
    ','denh22{1}');
34
35 set_param('desertation2full2ss2/ffStep1','after','1')
36 set_param('desertation2full2ss2/naStep2','after','0')
37 set_param('desertation2full2ss2/d1','after','0')
38 set_param('desertation2full2ss2/d2','after','0')
39
40 sim( 'desertation2full2ss2' )
41 figure
42 p=plot(tout,T1simout,'b--',tout,w2simout,'b-','LineWidth',2)
43 legend('T temperature','w angular speed')
44 xlabel('time (sec)')
45 ylabel('output Response')
46 title('system response conventional H inf(f.f.=1 & n.a.=0)')
47 grid on
48 figure
49
50 set_param('desertation2full2ss2/ffStep1','after','0')
51 set_param('desertation2full2ss2/naStep2','after','1')
52 sim( 'desertation2full2ss2' )
53 p=plot(tout,T1simout,'b--',tout,w2simout,'b-','LineWidth',2)
54 legend('T temperature','w angular speed')
55 xlabel('time (sec)')
56 ylabel('output Response')
57 title('system response conventional H inf(f.f.=0 & n.a.=1)')
58 grid on
59
60 figure
61 set_param('desertation2full2ss2/ffStep1','after','0')

```

```

62 set_param('desertation2full2ss2/naStep2','after','0')
63 set_param('desertation2full2ss2/d1','after','1')
64 set_param('desertation2full2ss2/d2','after','0')
65 sim( 'desertation2full2ss2' )
66
67 p=plot(tout,T1simout,'b--',tout,w2simout,'b-','LineWidth',2)
68 legend('T temperature','w angular speed')
69 xlabel('time (sec)')
70 ylabel('output Response')
71 title('system response conventional H inf(ff=0,na=1,d1=1,d2=0)')
72 grid on
73
74 figure
75 set_param('desertation2full2ss2/ffStep1','after','0')
76 set_param('desertation2full2ss2/naStep2','after','0')
77 set_param('desertation2full2ss2/d1','after','0')
78 set_param('desertation2full2ss2/d2','after','1')
79 sim( 'desertation2full2ss2' )
80
81 p=plot(tout,T1simout,'b--',tout,w2simout,'b-','LineWidth',2)
82 legend('T temperature','w angular speed')
83 xlabel('time (sec)')
84 ylabel('output Response')
85 title('system response conventional H inf(ff=0,na=1,d1=0,d2=1)')
86 grid on

```

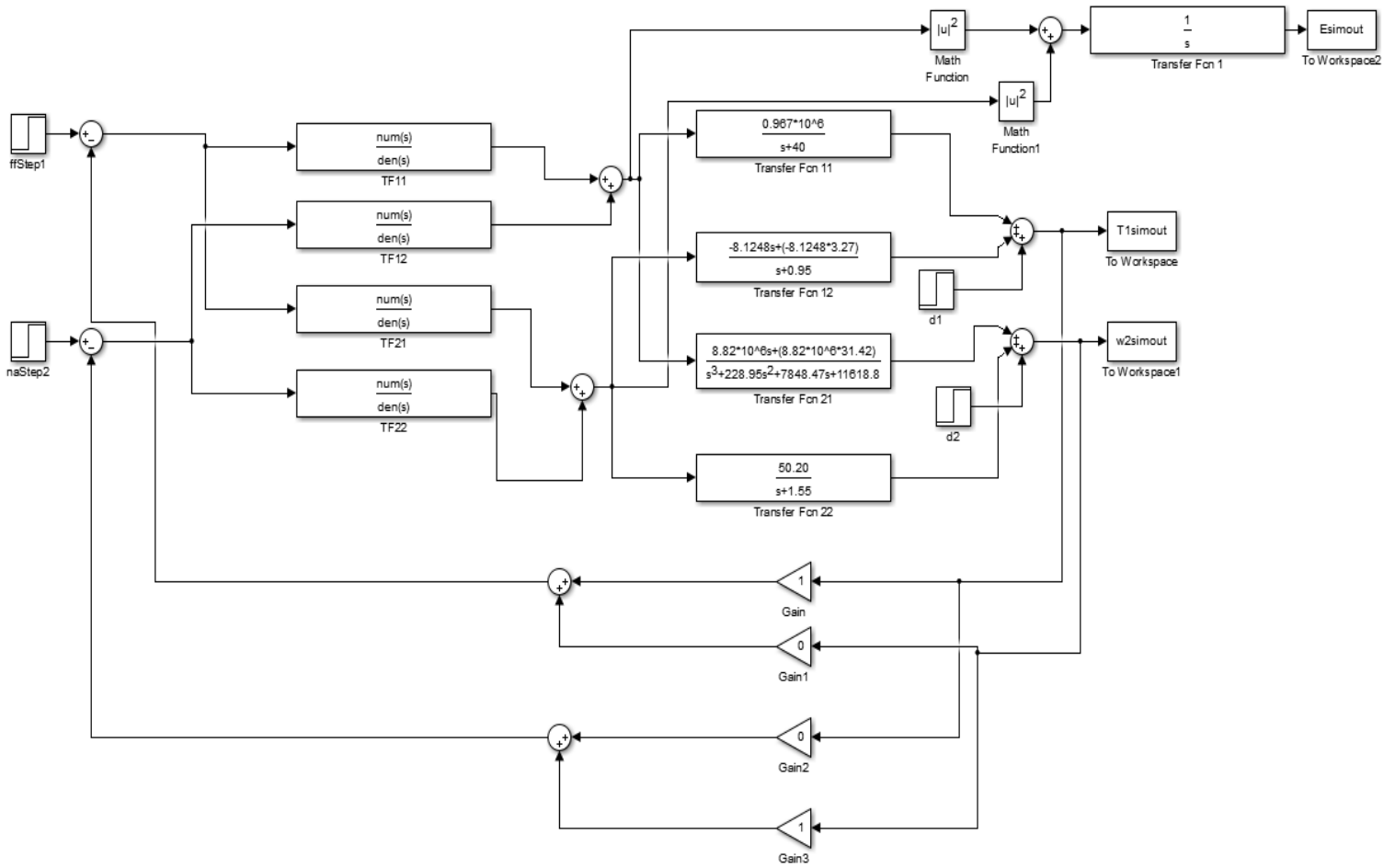


Figure A.2: H-infinity controller simulation model